Determinations of rational Dedekind-zeta invariants of hyperbolic manifolds and Feynman knots and links

J. M. Borwein[a] and D. J. Broadhurst[b]

Abstract   We identify 998 closed hyperbolic 3-manifolds whose volumes are rationally related to Dedekind zeta values, with coprime integers a and b giving

$$\frac{a}{b}\operatorname{vol}(\mathcal{M}) = \frac{(-D)^{3/2}}{(2\pi)^{2n-4}}\frac{\zeta_K(2)}{2\zeta(2)}$$

for a manifold $\mathcal{M}$ whose invariant trace field K has a single complex place, discriminant D, degree n, and Dedekind zeta value $\zeta_K(2)$. The largest numerator of the 998 invariants of Hodgson–Weeks manifolds is, astoundingly, $a = 2^4 \times 23 \times 37 \times 691 = 9,408,656$; the largest denominator is merely $b = 9$. We also study the rational invariant a/b for single-complex-place cusped manifolds, complementary to knots and links, both within and beyond the Hildebrand–Weeks census. Within the censi, we identify 152 distinct Dedekind zetas rationally related to volumes. Moreover, 91 census manifolds have volumes reducible to pairs of these zeta values. Motivated by studies of Feynman diagrams, we find a 10-component 24-crossing link in the case $n = 2$ and $D = -20$. It is one of 5 alternating platonic links, the other 4 being quartic. For 8 of 10 quadratic fields distinguished by rational relations between Dedekind zeta values and volumes of Feynman orthoschemes, we find corresponding links. Feynman links with $D = -39$ and $D = -84$ are missing; we expect them to be as beautiful as the 8 drawn here. Dedekind-zeta invariants are obtained for knots from Feynman diagrams with up to 11 loops. We identify a sextic 18-crossing positive Feynman knot whose rational invariant, $a/b = 26$, is 390 times that of the cubic 16-crossing non-alternating knot with maximal D_9 symmetry. Our results are secure, numerically, yet appear very hard to prove by analysis.

[a]) CECM, Simon Fraser University, Burnaby, B.C. V5A 1S6, Canada;
jborwein@cecm.sfu.ca; http://www.cecm.sfu.ca/~jborwein
[b]) Physics Department, Open University, Milton Keynes MK7 6AA, UK;
D.Broadhurst@open.ac.uk; http://physics.open.ac.uk/~dbroadhu

1 Introduction

This paper began with a study of hyperbolic links whose complementary volumes result from evaluations of Feynman diagrams [1]. For each of these volumes we found, by empirical means, a *closed–form* evaluation in terms of a few Clausen functions, evaluated at rational multiples of π. Then, thanks to generous advice from Don Zagier, we came to appreciate that these results form part of a much larger scaffold, whose unifying feature is the existence of rational relations between hyperbolic volumes and Dedekind zeta values. While the existence of such relations is understood [2, 3, 4], their precise forms appear to be unpredictable, thus far, by deductive mathematics. They are therefore ripe for the application of experimental mathematics. The work reported herein has involved a – to the authors – quite intoxicating mix of tools, allowing conjectures to be tested against known data and rapidly confirmed or rejected as the research progressed. We will return to these methodological issues in the conclusion.

For any single-complex-place field K, with discriminant D and degree n, we define

$$Z_K := \frac{(-D)^{3/2}}{(2\pi)^{2n-4}} \frac{\zeta_K(2)}{2\zeta(2)} \tag{1}$$

where the Dedekind zeta value $\zeta_K(2)$ is the sum of the inverse squares of the norms of the ideals [5, 6] of K, and $\zeta(2) := \sum_{n>0} 1/n^2 = \pi^2/6$ is the corresponding Riemann zeta value. It follows from [2] that Z_K is reducible, with unspecified[1] rational coefficients, to Bloch–Wigner dilogarithms $\{D(z_k) \mid z_k \in K\}$. The volume of a hyperbolic manifold, for which the single-complex-place field K is the invariant trace field [7], is systematically [8] reducible to such dilogarithms and, moreover, is expected to be some unspecified rational multiple of the very specific construct (1). Accordingly, we seek coprime integers a and b such that

$$\frac{a}{b} \operatorname{vol}(\mathcal{M}) = Z_K \tag{2}$$

for a manifold $\mathcal{M}$ with a single-complex-place invariant trace field K. We call a/b the rational Dedekind-zeta invariant of $\mathcal{M}$. It evaluates to unity for manifold m003$(-3,1)$, of conjecturally smallest volume. It will be seen to take some remarkable values.

In Section 2, we report findings of the rational invariant for 998 closed manifolds.

In Section 3, we find a further 12 single-complex-place fields from cusped manifolds, and compute corresponding rational invariants. We also identify 91 census manifolds whose volumes are reducible to *pairs* of Dedekind zeta values.

Section 4 concerns links, with complementary manifolds of a richer structure than those recorded in the Hildebrand–Weeks [9, 10] census of cusped manifolds triangulated by no more than 7 tetrahedra. In particular we identify a 24-crossing 10-component link, triangulated by 54 ideal tetrahedra with shapes in the quadratic field $\mathbf{Q}(\sqrt{-5})$ and determine its rational Dedekind-zeta invariant. We call it a platonic link, since its 10 components mimic the vertices and edges of a tetrahedron. The remaining 4 platonic

---

[1]Ratios of coefficients may be specified; here we ask for values.

links, similarly modelled on perfect solids, are shown to be quartic, after processing the 950 ideal tetrahedra from their triangulations.

Section 5 concerns connections [1, 11, 12, 13, 14] between Feynman diagrams, knots and links. Recent results [1] from quantum field theory suggested a connection between Dedekind zeta values and volumes of orthoschemes. We find 10 quadratic fields that forge such connections and in 8 cases now know links that have corresponding rational Dedekind-zeta invariants. The remaining 2 cases are quadratic fields with discriminants $D = -39$ and $D = -84$; these await the discovery of corresponding Feynman links. Hyperbolic knots with up to 18 crossings, from Feynman diagrams with up to 11 loops, are also analyzed. For crossing numbers greater than 9, the physics in [11, 12, 13, 14] is a more fertile source of Dedekind zeta values than an analysis of the maximally symmetric knots found in [15].

Section 6 offers some conclusions and suggestions for further study.

2 Dedekind-zeta invariants of closed manifolds

We have found rational Dedekind-zeta invariants for 998 manifolds in the Hodgson–Weeks census, which lists $11,031$ closed orientable manifolds, with 9,218 distinct volumes, all less than 6.5, and with all their geodesics having lengths greater than 0.3. These 998 manifolds have 224 distinct volumes, which are rationally related, via (1,2), to 140 distinct Dedekind zeta values, each corresponding to an invariant trace field of at least one census manifold. Table 1 enumerates the fields by degree. Tables 2–12 give, for each field K, a generating polynomial, together with its discriminant and the rational relation of Z_K to the volume of the first manifold in the census with invariant trace field K. The 224 distinct volumes are given in Tables 13a–f, where it can be observed that numerators and denominators of the 998 invariants are bounded by $a \leq 9408656$ and $b \leq 9$. Our methods were as follows.

2.1 Examination of 1,200 single-complex-place fields

It became clear, from studying [16, 17, 18, 19], that there are unspecified rational relations of the form (2) between Dedekind zeta values and volumes of some, but not all, of the manifolds in the Hodgson–Weeks census. We soon found that 30 of the first 32 census manifolds have rational Dedekind-zeta invariants, with $a \leq 46$ and $b \leq 3$. The 2 exceptions are manifolds m003$(-4, 1)$ and m004$(+7, 1)$, whose invariant trace fields have 2 complex places.

The next step was to obtain systematic listings of fields with precisely one complex place. Thanks to the `numberfields` directory[2] at the University of Bordeaux, we found files that order single-complex-place fields, for each degree $n \leq 7$, by the magnitudes, $-D$, of the discriminant. We selected the first 200 fields for each degree $n \in \{2, 3, 4, 5, 6, 7\}$ and used the `zetak` command of Pari to compute 19 digits of the Dedekind zeta values, $\zeta_K(2)$,

---

[2]`ftp://megrez.math.u-bordeaux.fr/pub/numberfields`

of these 1,200 fields. Forming Z_K, defined in (1), we made $1200 \times 11031 = 13,237,200$ indiscriminate comparisons between these target fields and the census entries. This took 19 seconds on a 233MHz Pentium. We found 842 manifolds, with 175 distinct volumes, rationally related to 96 distinct Dedekind zeta values, with numerators and denominators of the rational invariants bounded by $a \leq 46$ and $b \leq 5$.

Since the census provided 17-digit volumes, the probability of any of these simple rational results being spurious is comfortably less than 10^{-12}. Conversely, one needs only 5-digit precision for the volume to discover the rational Dedekind-zeta invariant in these 842 cases, and hence to obtain an accurate volume from (1). Only for degrees $n \geq 8$ do precision, core memory and CPUtime become issues. In the $n = 12$ case of Table 12, with $|D| = 12,476,239,474,594,496$, these issues require close attention.

The 96 fields that were caught by this 19-second trawl comprise all those of Tables 2 and 3 and all those above the lines drawn in Tables 4–7. Below the lines, and in Tables 8–12, we took assistance from Melbourne [7].

2.2 Examination of 44 fields found by Snap

For the remaining $140 - 96 = 44$ results of Tables 2–12, we made reference to the impressive body of files[3] at the University of Melbourne. These were obtained by Coulson, Goodman, Hodgson and Neumann [7] (hereafter referred to as CGHN) using 50-digit precision, in marked distinction to the 5 digits which suffice for the findings above.

CGHN make no reference to Dedekind zeta values; they do, however, find single-complex-place invariant trace fields for about 9% of the Hodgson–Weeks manifolds. The next step was to examine the overlap between our single-complex-place fields and theirs. We found that the CGHN file `closed_census_algebras` contains 95 of our 96 single-complex-place fields. The exception was the quintic field with $D = -14103$, for which our low-precision method had readily yielded the rational invariant $a/b = 2$ of the manifold s784(+5, 2), which was absent from the file `closed_census_algebras`, obtained by CGHN from 50-digit searches for fields of degree[4] not exceeding 16. We then referred to the file `closed.fields`, where s784(+5, 2) indeed appears, with the expected invariant trace field, $x^5 - 2x^4 + 2x^3 - x^2 - 2x - 1$.

Thus assured that all our 96 finds were genuine, we extracted all of the invariant trace fields from the CGHN files `closed_census_algebras` and `closed.fields`, and asked Pari to determine their signatures and discriminants. This revealed 44 cases beyond the ranges of our search, namely the 32 below the lines in Tables 4–7 and the 12 in Tables 8–12. Within our selected ranges, CGHN had found all and only our 96 single-complex-place fields, indicating the reliability of both their methods and ours.

The next step was obvious, yet computationally demanding: to determine rational Dedekind-zeta invariants for the manifolds associated by Snap to the remaining 44 large-discriminant single-complex-place fields. The `zetak` command of Pari was entirely ade-

---

[3]http://www.ms.unimelb.edu.au/~snap
[4]We later ran Snap at 100-digit precision, and found a group field of degree 20.

quate to complete Tables 4–7, at 19-digit precision, yielding numerators and denominators bounded by $a \leq 976$ and $b \leq 5$, for which merely 7-digit precision would have been amply sufficient. The 12 fields of Tables 8–12 presented a much tougher computational challenge.

At degree $n = 8$, Pari-GP 2.0.11 began to falter, with `zetak` yielding results drastically below the requested precision (as warned in the Pari manual) or running out of memory (when allocated 100MB of core). Accordingly we devised a method based on the `dirzetak` command, which returns the multiplicities, $m_K(n)$, of the ideals of K with norm n, up to some requested maximum, N, that may comfortably extend to $N = 10^6$. These multiplicities are the numerators of the Dirichlet series

$$\zeta_K(2) = \sum_{n>0} \frac{m_K(n)}{n^2} \tag{3}$$

We then computed the truncated sums $S_N := \sum_{n=1}^{N} m_K(n)/n^2$, and accelerated their convergence by forming $T_{N,M} := (S_N N - S_M M)/(N - M)$, with $M \approx \frac{1}{2}N$. This removes a predictable $O(1/N)$ truncation error, leaving an $O(1/N^{3/2})$ "random-walk" error. With $N \leq 10^6$, we were able to achieve 10-digit precision, by averaging out fluctuations in $T_{N,M}$. Even in the most demanding case of Table 12, where the rational invariant is a 7-digit integer, we were left with 3 vanishing decimal places for $a/b = 9408656.000 \pm 0.001$.

Hence we completed the task for Hodgson–Weeks manifolds. Tables 2–12 give 140 single-complex-place invariant trace fields of closed census manifolds, of which 96 were detected by us without reference to CGHN. The 224 distinct census volumes rationally related to the Dedekind zeta values of these fields are given in Tables 13a-f. These 224 distinct volumes correspond to 998 of the 11,031 entries of the Hodgson–Weeks census file `ClosedManifolds` available[5] from the Geometry Center at the University of Minnesota.

2.3 A special case: manifold v3066$(-1, 2)$

We note a peculiarity of manifold v3066$(-1, 2)$, with the same volume as v3066$(+1, 2)$. The latter has unit Dedekind-zeta invariant and hence a volume

$$Z_{K_+} := \frac{59^{3/2}}{(2\pi)^2} \frac{\zeta_{K_+}(2)}{2\zeta(2)} = 5.13794120187341776984134 8339 \ldots \tag{4}$$

where the cubic invariant trace field of v3066$(+1, 2)$ is

$$K_+ := x^3 + 2x - 1 \tag{5}$$

with discriminant -59. Snap, working at 100-digit precision, gave the invariant trace field of v3066$(-1, 2)$ as a join of (5) with $\mathbf{Q}(\sqrt{-59})$, generated by a root of the sextic

$$K_- := x^6 - 3x^5 + 10x^4 - 15x^3 + 21x^2 - 14x + 4 \tag{6}$$

with discriminant $(-59)^3$ and 3 complex places. The Borel regulator [7, 20] of v3066$(-1, 2)$ was given as $\left[Z_{K_+}, -\frac{1}{2}Z_{K_+}, -\frac{1}{2}Z_{K_+} \right]$. It thus appears that a single-complex-place invariant trace field is sufficient, yet *not* necessary, to give a rational Dedekind-zeta invariant.

---

[5] The 1995 file `ftp://ftp.geom.umn.edu/pub/software/snappea/tables/ClosedManifolds` contains 11,031 entries; unfortunately some of the Dehn fillings do not correspond to those packaged, internally, with SnapPea. We enlisted Snap, to check all the surgeries given in Tables 2–13.

2.4 How may one *derive* the rational invariant?

Some of our results contain non-trivial factors, with 4-digit and 3-digit primes in $3 \times 1223 = 3669$ and $2^4 \times 3 \times 5 \times 967 = 232,080$, from Table 10, and $2 \times 3 \times 7 \times 11 \times 149 = 68,838$, from Table 11. Their origins are obscure. The duodecadic example of Table 12 entails $a/b = 2^4 \times 23 \times 37 \times 691 = 9,408,656$. We note, though cannot explain, the circumstance that its largest prime factor also occurs in $\zeta(12)/\pi^{12} = \frac{691}{638512875}$. Reverse engineering gave 50 decimal places of

$$\zeta_{K_{12}}(2) \quad = \quad 1.06095699592540035751698213238632531266926282705990\ldots \qquad (7)$$
$$K_{12} \quad := \quad x^{12} - 3x^{11} - 8x^{10} + 17x^9 + 27x^8 - 19x^7 - 50x^6$$
$$- 24x^5 + 44x^4 + 37x^3 - 5x^2 - 8x - 1 \qquad (8)$$

from high-precision triangulation of manifold v2824(+4, 1). We know of no easy way to check (7) beyond the first 10 digits, confirmed by accelerated convergence of a million truncations of (3).

Arguments from K-theory [16, 19] appear powerless to derive values for the Dedekind-zeta invariant, a/b, though they imply [2, 3, 4] its rationality, for every manifold whose invariant trace field has a single complex place. It thus remains a challenge to derive the simple value $a/b = 4$, for the quadratic manifold m036($-4, 3$), with invariant trace field $\mathbf{Q}(\sqrt{-7})$ and volume observed, at 1800-digit precision, to coincide with

$$\frac{1}{4} Z_{\mathbf{Q}(\sqrt{-7})} \quad = \quad \frac{7}{4} \left\{ \mathrm{Cl}_2 \left(\frac{2\pi}{7} \right) + \mathrm{Cl}_2 \left(\frac{4\pi}{7} \right) - \mathrm{Cl}_2 \left(\frac{6\pi}{7} \right) \right\} \qquad (9)$$
$$= \quad 2.6667447834490597907967124626106500440983838885526 3\ldots \quad (10)$$

whose reduction to

$$\mathrm{Cl}_2(\theta) := \sum_{n>0} \frac{\sin(n\theta)}{n^2} \qquad (11)$$

is derived in Section 4. Triangulation gives

$$\mathrm{vol}(\mathrm{m036}(-4, 3)) \quad = \quad 2D \left(-e^{-i\theta_7} \right) + D \left(-\tfrac{1}{2} e^{-i\theta_7} \right) \qquad (12)$$
$$\theta_7 \quad := \quad 2 \arctan \sqrt{7} \qquad (13)$$

where the Bloch–Wigner dilogarithm

$$D(z) := \Im \mathrm{Li}_2(z) + \log|z| \Im \log(1-z) = \Im \sum_{n>0} \left(\frac{1}{n^2} - \frac{\log|z|}{n} \right) z^n \qquad (14)$$

gives the volume of an ideal tetrahedron whose essential dihedral angles are the arguments of $\{z, 1/(1-z), 1-1/z\}$. The 1800-digit agreement of (12) with (9) is compelling evidence that, with $\theta_7 := 2 \arctan \sqrt{7}$,

$$\frac{3}{2} \mathrm{Cl}_2(\theta_7) - \frac{3}{2} \mathrm{Cl}_2(2\theta_7) + \frac{1}{2} \mathrm{Cl}_2(3\theta_7) = \frac{7}{4} \left\{ \mathrm{Cl}_2 \left(\frac{2\pi}{7} \right) + \mathrm{Cl}_2 \left(\frac{4\pi}{7} \right) - \mathrm{Cl}_2 \left(\frac{6\pi}{7} \right) \right\} \qquad (15)$$

An elementary proof of this remarkable relation between Clausen values has escaped both us, and also, it appears, the authors of [16, 17, 18, 19]. To cast it in a less classical form, we multiply (15) by 2, and transform to Bloch–Wigner functions, obtaining

$$4\,D\left(\frac{3+i\sqrt{7}}{4}\right) + 2\,D\left(\frac{3+i\sqrt{7}}{8}\right) = 7\,D\left(2\frac{1+i\tan\frac{\pi}{7}}{3-\tan^2\frac{\pi}{7}}\right) \tag{16}$$

where the argument on the r.h.s. is a root of the totally complex sextic

$$K_6 := x^6 - 4x^5 + 9x^4 - 8x^3 + 4x^2 - 2x + 1 \tag{17}$$

with discriminant $(-7)^5$. The l.h.s. of (16) is the volume of the cusped manifold s776, which is complementary to the 3-component 6-crossing link 6_1^3. Its triangulation immediately yields 6 ideal tetrahedra, with 2 distinct shapes in the quadratic field $\mathbf{Q}(\sqrt{-7})$. The challenge is to prove that by combining these 6 one forms the same volume as from the 7 congruent sextic shapes on the r.h.s. of (16). This is a modern version of our puzzle (15) in classical analysis: how may one relate Clausen values at multiples of $\theta_7 := 2\arctan\sqrt{7}$ to Clausen values at multiples of $2\pi/7$, when there appears to be no non-trivial relation between trigonometric functions of the two sets of angles? A far greater challenge would be to derive, rather than merely measure, the integer Dedekind-zeta invariant $2^4 \times 23 \times 37 \times 691$ of the closed manifold v2824($+4, 1$).

3   Cusped manifolds and join fields

Now we turn to the study of cusped manifolds, complementary to knots and links. Packaged with SnapPea [21], there are the 4,815 orientable cusped manifolds of the Hildebrand–Weeks census [9], triangulated by no more than 7 ideal tetrahedra, and 114 non-orientable manifolds, triangulated by no more than 5. Making 4929×1200 comparisons with the Dedekind zeta values of Section 2.1, we found 7 new single-complex-place fields, beyond those from the Hodgson–Weeks census. Then the CGHN file `cusped.fields` confirmed these finds and yielded the remaining 5 fields of Table 14, with larger discriminants. In Table 14, we give the rational Dedekind-zeta invariant of a selected cusped manifold for each of the 12 new fields.

Our tally of single-complex-place fields is now $96 + 44 + 7 + 5 = 152$. Among the 4,929 cusped manifolds, we found 312 whose volumes are rationally related to one of the 152 Dedekind zeta values, with numerators and denominators in (2) bounded by $a \le 2853$ and $b \le 7$.

We also sought integer relations of the form

$$a\,\mathrm{vol}(\mathcal{M}) = b_1 Z_{K_1} + b_2 Z_{K_2} \tag{18}$$

corresponding to a cusped or closed manifold $\mathcal{M}$ whose invariant trace field is the join of single-complex-place fields K_1 and K_2, or is a subfield of this join. Restricting K_1 and K_2 to the 152 fields of Tables 2–12 and Table 14, we found 91 census manifolds, with 26

6

distinct volumes, rationally related, via (18), to pairs of Dedekind zeta values. Details of the 29 cusped and 62 closed manifolds are provided by Tables 15–18. Two of the 26 integer relations entail join fields noted in [7], namely the first in Table 16 and the second in Table 17. We used Pari's `nfisincl` command to confirm that all 6 of the quartic invariant trace fields in Table 18 are subfields of the octadic joins. In 4 of these 6 cases, distinct values of b_1/b_2 occur, for the same invariant trace field.

We believe that we have exhausted the 3-term relations between census volumes and pairs of the 152 target Dedekind zeta values. David Bailey's impressively efficient, arbitrary precision [22], implementation of PSLQ [23] found the 91 relations in 40 minutes and then took 17 hours to exhaust the $(4815 + 114 + 11031) \times \binom{152}{2} = 183,156,960$ indiscriminate possibilities. The PSLQ search rate was thus a healthy 3 kHz. No reduction to 3 distinct Dedekind zeta values was detected, presumably because the census volumes are kept deliberately small.

4 Links whose volumes link Clausen values

Our order of presentation is the reverse of the order in which we obtained results. Our primary motivation was to elucidate connections between Clausen values, revealed by studies of Feynman diagrams [1], on which we comment in Section 5.

This section concerns links whose rational Dedekind-zeta invariants link Clausen values. An example is provided by the attractive alternating[6] link of Fig. 1, discovered as a result of work on light-by-light scattering, reported in Section 5. A second is provided by the non-alternating[7] daisy-chain link of Fig. 2. These form part of our study of Dedekind-zeta invariants of quadratic links.

Next in chronological sequence, came the higher-degree Dedekind-zeta invariants of cusped manifolds, in Section 3. Finally, we undertook the systematic study of closed manifolds, culminating with the 12th-degree Dedekind-zeta invariant of Section 2. Like most stories, it benefits from signposting.

4.1 Signpost: integer sequence A003657

Mathematically speaking, the results of Section 2, while numerically striking, are of a rational character [2, 3, 4] that was expected by specialists of K-theory (which we are not). The challenge is not to understand why a rational Dedekind-zeta invariant exists, but to learn how to derive (as opposed to measure) it. The cusped results of Section 3 were of the same character as for closed manifolds: hyperbolic knots and links have rational Dedekind-zeta invariants if their complementary cusped manifolds have single-complex-place invariant trace fields. Here, in Section 4, we address the question raised by the sparsity of quadratic entries in Tables 2 and 14: where are the quadratic links with

---

[6]The viewer is asked to alternate all the crossings in Fig. 1 and Figs. 3–8.
[7]The viewer is asked to supply the uniquely non-alternating non-trivial crossings in Fig. 2.

(negated) discriminants beyond the first 4 entries in the integer sequence A003657 of Neil Sloane's on-line encyclopedia[8]

$$\underline{3}, \underline{4}, \underline{7}, \underline{8}, \underline{11}, \underline{15}, 19, \underline{20}, 23, \underline{24}, 31, 35, \underline{39}, 40, 43, 47, 51, 52, 55, 56, 59, 67, 68, 71, 79, 83, \underline{84} \ldots \tag{19}$$

Only the first 4 cases figure in the Hildebrand–Weeks census. Here we identify 4 more underlined cases, with $-D \in \{11, 15, 20, 24\}$, where the platonic link of Fig. 1 furnishes an example with $D = -20$, and the daisy-chain link of Fig. 2 furnishes an example with $D = -24$. Then, in Section 5, we shall explain how we were led to Figs. 1 and 2, by consideration of the physical process of light-by-light scattering, and why its Feynman diagrams suggest that the remaining 2 underlined cases, with $D = -39$ and $D = -84$, will be of similar symmetrical appeal, and similar analytical mystery.

4.2 Dirichlet character

The simplest example of a number field with a single complex place is an imaginary-quadratic field $\mathbf{Q}(\sqrt{-d})$, where d is a square-free positive integer. When $d \equiv 3 \pmod 4$, the discriminant is $D = -d$; otherwise it is $D = -4d$.

It is proven in [24] that

$$\frac{\zeta_K(2)}{\zeta(2)} = \sum_{n>0} \frac{\chi_K(n)}{n^2} \tag{20}$$

where χ_K is the real Dirichlet character of the group of units of the field $\mathbf{Z}/|D|$ and D is the discriminant of the imaginary-quadratic field K. The Dirichlet character is related to the Jacobi (or Kronecker) symbol by

$$\chi_K(n) = \left(\frac{D}{n}\right) \tag{21}$$

which vanishes if $\gcd(D, n) > 1$. When D is odd, one may use the alternative form $\left(\frac{n}{|D|}\right)$.

Using (20) in (1), at $n = 2$, one happily disposes of powers of π. We dispose of $\sqrt{-D}$, by using the imaginary-quadratic result [24]

$$\sum_{n>0} \frac{\chi_K(n)}{n^2} = \frac{1}{\sqrt{-D}} \sum_{-D>k>0} \chi_K(k) \mathrm{Cl}_2 \left(\frac{2\pi k}{|D|}\right) \tag{22}$$

which yields a finite sum over the elements of the group of units. Finally, we dispose of a factor 2, via the reflection relations $\chi_K(k) = -\chi_K(|D| - k)$ and $\mathrm{Cl}_2(\theta) = -\mathrm{Cl}_2(2\pi - \theta)$, to obtain the readily computable result

$$Z_K = Z_{|D|} := D \sum_{-D>2k>0} \left(\frac{D}{k}\right) \mathrm{Cl}_2 \left(\frac{2\pi k}{D}\right) \tag{23}$$

with the magnitude of the discriminant identifying the imaginary-quadratic field.

---

[8]http://www.research.att.com/~njas/sequences

Thanks to David Bailey [22], it is now a routine matter to evaluate (23) to high precision[9], using [25]

$$\frac{\mathrm{Cl}_2(\theta)}{\theta} = 1 - \tfrac{1}{2}\log(\theta^2) + \sum_{n=1}^{\infty} \frac{\zeta(2n)}{2n^2+n}\left(\frac{\theta}{2\pi}\right)^{2n} \tag{24}$$

which converges faster than $1/9^n$, for $\theta \in [0, 2\pi/3]$. An angle in $[2\pi/3, \pi]$ may be transformed to a pair in $[0, 2\pi/3]$, by rearrangement of the duplication formula

$$\tfrac{1}{2}\mathrm{Cl}_2(2\theta) = \mathrm{Cl}_2(\theta) - \mathrm{Cl}_2(\pi - \theta) \tag{25}$$

Rather than compute $\zeta(2n)/(2\pi)^{2n} = \tfrac{1}{2}|B_{2n}|/(2n)!$ recursively, from the Bernoulli numbers, we used a FFT program written by David Bailey to evaluate $\{\zeta(2n) \mid 0 \leq n < 2^m\}$, in one fell swoop, by a multi-dimensional generalization of Newton's method. With $m = 11$, the initial outlay, to tabulate 2048 coefficients to 1800 digits, was 8 minutes; then 1800 good digits of any Clausen value in $\{\mathrm{Cl}_2(\theta) \mid 0 < \theta < 2\pi/3\}$ are obtainable in less than 2 seconds on a 533MHz machine. Low-precision results for $Z_{|D|}$ are given in Table 19.

It follows from (23) that every discovery of a rational Dedekind-zeta invariant for a quadratic link gives a relation between a set of Clausen values at angles whose tangents involve $\sqrt{d}$, and a set of Clausen values at angles which are multiples of $2\pi/|D|$. We have already seen this, rather strikingly, in the case $-D = d = 7$ of (15), where the hyperbolic 6-crossing 3-component link[10] 6_1^3 mediates between Clausen values, and hence the Bloch–Wigner dilogarithms of (16), with very different types of argument on the left and right.

We now address the question: which links have volumes that link Clausen values?

4.3   Figure-8 knot at $D = -3$

The first case, at $D = -3$, is elementary. The unique[11] arithmetic knot is the figure-8 knot of Fig. 3. Its volume is the first entry of Table 19. It links Clausen values at $2\arctan\sqrt{3}$ and $2\pi/3$. This relation clearly poses no analytical puzzle, since the angles are identical.

4.4   Whitehead link at $D = -4$

Just as the simplest hyperbolic knot, 4_1, gave the answer at $D = -3$, so the simplest hyperbolic 2-component link, namely the Whitehead link 5_1^2 of Fig. 4, gives the answer at $D = -4$. Its volume is the second entry of Table 19. It links Clausen values at $2\arctan\sqrt{1}$ and $2\pi/4$, which are again identical.

---

[9]http://science.nas.nasa.gov/Groups/AAA/db.webpage/mpdist/mpdist.html

[10]We use the notation of [26], whose appendix give drawings of links up to 9 crossings.

[11]See Helaman Ferguson's sculpture at http://www.mtholyoke.edu/acad/math/ma/sculpture.htm

4.5 Link 6_1^3 at $D = -7$

The Dedekind-zeta invariant of the link 6_1^3, illustrated in Fig. 5, is measured to be 2, corresponding to

$$2\left\{3\mathrm{Cl}_2(\theta_7) - 3\mathrm{Cl}_2(2\theta_7) + \mathrm{Cl}_2(3\theta_7)\right\} = Z_7 = 7\left\{\mathrm{Cl}_2\left(\frac{2\pi}{7}\right) + \mathrm{Cl}_2\left(\frac{4\pi}{7}\right) - \mathrm{Cl}_2\left(\frac{6\pi}{7}\right)\right\} \quad (26)$$

with $\theta_7 := 2\arctan\sqrt{7}$. At 1800-digit precision, PSLQ finds this to be the sole integer relation between the 6 Clausen values. The combination on the left is selected by hyperbolic geometry; that on the right by the Dirichlet character. Thus the rational Dedekind-zeta invariant of link 6_1^3 encodes a highly non-trivial analytical relation between Clausen values. A derivation of $a/b = 2$ would prove (26). Conversely, a proof of (26) would derive $a/b = 2$. Where may one find *any* such proof?

4.6 Link 9_{40}^2 at $D = -8$

As exemplar of the next non-trivial relation between Clausen values, we select the 9-crossing 2-component link $9_{40}^2 := (\sigma_1^2\sigma_2^{-1})^3$ of Fig. 6. Its Dedekind-zeta invariant is observed to be unity, which implies that its volume is equal to each side of

$$\tfrac{1}{2}\left\{27\mathrm{Cl}_2(\theta_2) - 9\mathrm{Cl}_2(2\theta_2) + \mathrm{Cl}_2(3\theta_2)\right\} = Z_8 = 8\left\{\mathrm{Cl}_2\left(\frac{2\pi}{8}\right) + \mathrm{Cl}_2\left(\frac{6\pi}{8}\right)\right\} \quad (27)$$

with $\theta_2 := 2\arctan\sqrt{2}$. As in the case of (26), a proof is lacking.

4.7 A 12-crossing 4-component link at $D = -11$

In [7] it was noted that neither the closed nor the cusped census entails the field $\mathbf{Q}(\sqrt{-11})$. In [1] it was observed that the 12-crossing 4-component link of Fig. 7, with braid word $(\sigma_1\sigma_2^{-2}\sigma_3\sigma_2^{-2})^2$, entails this field. Its Dedekind-zeta invariant is observed to be unity, corresponding to the relation

$$15\mathrm{Cl}_2(\theta_{11}) - 10\mathrm{Cl}_2(2\theta_{11}) + \mathrm{Cl}_2(5\theta_{11}) = Z_{11} = 11\sum_{k=1}^{5}\left(\frac{k}{11}\right)\mathrm{Cl}_2\left(\frac{2\pi k}{11}\right) \quad (28)$$

where $\theta_{11} := 2\arctan\sqrt{11}$ and $\left(\frac{k}{11}\right)$ is the Jacobi (or Legendre) symbol for the Dirichlet character. Again, we lack a proof.

4.8 A 12-crossing 3-component link at $D = -15$

The next case likewise comes from [1]. The 12-crossing 3-component link of Fig. 8, with braid word $(\sigma_1^2\sigma_2^{-2})^3$, has Dedekind-zeta invariant empirically equal to 2, at 1800-digit precision. This corresponds to the relation

$$24\mathrm{Cl}_2(\theta_{5,3}) - 12\mathrm{Cl}_2(2\theta_{5,3}) - 8\mathrm{Cl}_2(3\theta_{5,3}) + 6\mathrm{Cl}_2(4\theta_{5,3}) = Z_{15} = 15\sum_{k=1}^{7}\left(\frac{k}{15}\right)\mathrm{Cl}_2\left(\frac{2\pi k}{15}\right) \quad (29)$$

with $\theta_{5,3} := 2 \arctan \sqrt{5/3}$. Again, where is the proof?

4.9 A self-dual platonic link at $D = -20$

The reader might now expect us to consider the case $D = -19$. For reasons that will be given in Section 5, we skip to $D = -20$, where we were rewarded by the splendidly symmetric alternating platonic link drawn in Fig. 1. Its Dedekind-zeta invariant was measured to be unity. This innocent-sounding statement translates to our 5th unproven relation

$$36\mathrm{Cl}_2(\theta_5) - 30\mathrm{Cl}_2(2\theta_5) + 4\mathrm{Cl}_2(3\theta_5) + 3\mathrm{Cl}_2(4\theta_5) = Z_{20} = 20 \sum_{k \in \{1,3,7,9\}} \mathrm{Cl}_2\left(\frac{2\pi k}{20}\right) \quad (30)$$

with $\theta_5 := 2 \arctan \sqrt{5}$. Between these 8 Clausen values, PSLQ found no other relation.

We found that, far from complicating the result, the 4 Clausen values on the left simplify the 54 Bloch–Wigner values of the triangulation in $\mathbf{Q}(\sqrt{-5})$. There is, of course, an infinity of rewritings of (30), obtained by adding, on the left, combinations of Bloch–Wigner values that algebraically [17] sum to zero, by virtue of special cases of the classical [25] 2-variable 5-dilogarithm relation of Abel, which is easily proved by differentiation. Here, as elsewhere, we expose the classical analysis that remains to be done.

4.10 A 48-crossing daisy-chain link at $D = -24$

The attentive reader will now expect us to skip the case $D = -23$ and jump to the 8th underlining in (19), at $D = -24$. This is precisely what we did, though the character of the result was not what we first supposed. It seemed to us that the hallmark of past success, in finding links that link Clausen values, was to achieve the largest possible symmetry group. What, we asked ourselves, could pack a better symmetry-to-crossing ratio than the remaining 4 platonic alternating links?

Let us denote the tetrahedral link of Fig. 1 by $T := 24_{\mathrm{tet}}^{10}$. The 4 non-self-dual alternating platonic links have components that mimic the vertices and edges of the cube $C := 48_{\mathrm{cub}}^{20}$, octahedron $O := 48_{\mathrm{oct}}^{18}$, dodecahedron $D := 120_{\mathrm{dod}}^{50}$, and icosahedron $I := 120_{\mathrm{ico}}^{42}$, where, for example, the last has 120 alternating crossings of its 42-components, which mimic the 12 vertices and 30 edges of the perfect solid with 20 faces. These links are highly symmetrical, yet none of their 4 volumes yielded the sought-for rational relation to a quadratic Dedekind zeta value. Later, we show that they are quartic links.

Instead, we found an answer to our 8th question by a more child-like construction: a non-alternating daisy chain. By a daisy chain we mean a link each of whose components has 2 crossings with a neighbour on one side, and 2 crossings with a neighbour on the other, with the whole forming a circle, as in Fig. 2. By a non-alternating daisy chain, we mean one in which the 4 crossings of each component occur in an order over-over-under-under, while still linking with neighbours. A little doodling should convince the reader that non-alternating daisy-chain links must have an even number of components.

A delightful feature of Jeff Weeks' program SnapPea [21] is that it enables one to draw such chains quickly, and then ask whether the resultant non-alternating link has quadratic shapes in its triangulation. Using A.C. Manoharan's port of SnapPea to Windows95[12], we inferred, from instances with up to 96 crossings, that the non-alternating daisy-chain link with $2n \geq 6$ components, and hence $4n \geq 12$ crossings, has hyperbolic volume

$$V_{2n} = 8nD\left(i\tan\frac{(n-2)\pi}{4n}\right) \tag{31}$$

The first 4 hyperbolic non-alternating daisy chains yield results with $-D \in \{3, 4, 8, 20\}$:

$$V_6 = 4Z_4 \tag{32}$$
$$V_8 = 2Z_8 \tag{33}$$
$$V_{10} = \tfrac{1}{2}Z_{20} + V_6 \tag{34}$$
$$V_{12} = 20Z_3 \tag{35}$$

Then nothing interesting happens until we reach 24 components, with 48 crossings, where

$$V_{24} = Z_{24} + V_8 \tag{36}$$

hits the target, at $D = -24$.

SnapPea illustrates this nicely. Drawing daisy chains with 6, 8, 10, 12, 24 components, and inspecting the triangulations, one detects the square roots of 1, 2, 5, 3, 6. The last, illustrated in Fig. 2, delivers a result for $Z_{24} = V_{24} - V_8$, namely

$$60\,\mathrm{Cl}_2(\theta_{3,2}) - 18\,\mathrm{Cl}_2(2\theta_{3,2}) - 4\,\mathrm{Cl}_2(3\theta_{3,2}) + 3\,\mathrm{Cl}_2(4\theta_{3,2}) = Z_{24} = 24\sum_{k \in \{1,5,7,11\}}\mathrm{Cl}_2\left(\frac{2\pi k}{24}\right) \tag{37}$$

with $\theta_{3,2} := 2\arctan\sqrt{3/2}$. So, for the 6th time, we have a relation that is as easy to check numerically as it appears hard to derive.

4.11 Quartic platonic links

Our first guess, that the 4 non-self-dual platonic links might yield quadratic number fields, failed. Nonetheless, it is interesting to determine their number fields, and hence obtain accurate volumes. This is clearly a taxing job. To prepare for it, we first tackled a problem of similar complexity, where an accurate answer could be inferred.

We found that by adding n concentric components at each of the 4 "vertices" of Fig. 1, one obtains a volume $Z_{20} + 2nZ_{15}$ for the link with $24 + 24n$ crossings and $10 + 4n$ components, when $n \leq 5$. At $n = 6$, SnapPea was given the 34-component link with 168 crossings, which was triangulated to give 632 ideal tetrahedra, each having a volume

---

[12]http://home.att.net/~Manoharan/SnapPea/snappea.html

$D(z_k)$ with $z_k \in \mathbf{Q}(\sqrt{-5})$ or $z_k \in \mathbf{Q}(\sqrt{-15})$. We output the 632 shapes, and computed, at 1800-digit precision, the $3 \times 632 = 1,896$ Clausen values entailed by

$$D(z) = V(\arg(z), -\arg(1-z)) \tag{38}$$
$$V(\theta_1, \theta_2) := \tfrac{1}{2}\left\{\mathrm{Cl}_2(2\theta_1) + \mathrm{Cl}_2(2\theta_2) - \mathrm{Cl}_2(2\theta_1 + 2\theta_2)\right\} \tag{39}$$

obtaining 1800-digit agreement with the expectation $Z_{20} + 12Z_{15} = 502.408032\ldots$ for the volume. This gave us confidence that we could process the 950 ideal tetrahedra entailed by the remaining 4 platonic links.

We obtained from SnapPea the low-precision volumes

$$\mathrm{vol}(C) \approx \mathrm{vol}(O) \approx 114.537611 \tag{40}$$
$$\mathrm{vol}(D) \approx \mathrm{vol}(I) \approx 310.913145 \tag{41}$$

from $128 + 130 + 346 + 346 = 950$ ideal tetrahedra.

The duality between cube and octahedron, and between dodecahedron and icosahedron, is gratifying. Such duality is not restricted to platonic links. More generally, suppose that we have a link, L, with an alternating projection in which the components may be separated into two classes: vertex (V) components and edge (E) components, with pairs of crossings only between V and E components, and every E connecting a pair of V's. Thus the crossing number is 4 times the number of E components. Now shrink the V components to true vertices (some of which may be divalent) and the E components to true edges that connect these points, to obtain a planar graph, P. Then construct the dual graph, P^*, whose vertices lie in the regions of the plane partitioned by the edges of P and whose edges thus cross the edges of P. Now thicken P^* to obtain the alternating link L^* dual to L. The crossing numbers of L and L^* are equal, but the numbers of components need not be. For example $C := 48^{20}_{\mathrm{cub}}$ has more components than $C^* := O := 48^{18}_{\mathrm{oct}}$, and $D := 120^{50}_{\mathrm{dod}}$ has more than $D^* := I := 120^{42}_{\mathrm{ico}}$. On the basis of these and further tests, we conjecture that $\mathrm{vol}(L) = \mathrm{vol}(L^*)$, for every shrinkable link L.

To identify the number fields of the $\{C, O\}$ and $\{D, I\}$ pairs, we first examined the cusp shapes, and found that

$$K_C := \mathbf{Q}\left(\sqrt{8\sqrt{2} - 15}\right) \tag{42}$$

gave a simple fit to the cusp shapes of $\{C, O\}$, at the 12-digit precision provided by SnapPea, while

$$K_D := \mathbf{Q}\left(\sqrt{-12\sqrt{5} - 31}\right) \tag{43}$$

similarly fitted the cusp shapes of $\{D, I\}$.

We then output z-values of the triangulations. Fitting these was not easy, since the data now consisted of numerical values, to 12 decimal places, of $1,900$ real or imaginary parts, each of which was supposed to be fittable by two powers of $\sqrt{15 - 8\sqrt{2}}$, in the cubical and octahedral cases, or $\sqrt{31 + 12\sqrt{5}}$, in the dodecahedral and icosahedral cases.

13

In each of the $1,900$ cases we required a significant integer relation between 3 numbers: the 12-digit SnapPea datum and the two powers, namely 0 and 2 for a real part, or 1 and 3 for an imaginary part. Whether this can be done by a reliable and uniformly automated method depends upon the largest integer. If it has more than 4 digits, the matter is moot, since fitting 12-digit data with 3 integers with up to 4 digits is already a parlous business. In fact our first attempt yielded garbage in a significant fraction of the $1,900$ cases.

Fortunately, 3 features of the mathematics enable us to crack this tough nut. First, the 6-fold symmetry of the Bloch–Wigner function

$$D(z) = D(1/(1-z)) = D(1 - 1/z) = D(1/\overline{z}) = D(1 - \overline{z}) = D(\overline{z}/(\overline{z} - 1)) \qquad (44)$$

gave us 6 bites at each cherry. Secondly, number theory suggested that we might do well to make the Ansatz

$$z = \frac{1}{I_z} \sum_{p=0}^{3} I_p u^p \qquad (45)$$

with $6 \times 950 \times 5 = 28,500$ integers relating 6 equivalent z values of 950 ideal volumes to 4 powers of $u = \frac{1}{2}(1 + i\sqrt{15 - 8\sqrt{2}})$ or $u = \frac{1}{2}(1 + i\sqrt{31 + 12\sqrt{5}})$. Finally, we were prepared for even the simplest of the 6 fits to any shape to contain the prime factor $97 = 15^2 - 2 \times 8^2$ of the cubical/octahedral discriminant, or $241 = 31^2 - 5 \times 12^2$ in the dodecahedral/icosahedral case.

These 3 features allowed us to devise a diversity of algorithms that yielded, eventually, total fits which we consider to be corporately indubitable. Our confidence came from a fourth mathematical feature, which at first sight appeared to make life difficult, namely that there was virtually no overlap between problems that were supposed to be related by duality. In fact we found only two distinct ideal volumes that contributed to both the dodecahedron and icosahedron, and each of these was unambiguous. The absence of further overlap doubled the computational load, yet made the resulting numerical agreement of volumes, to 1800 digits, a potent signal of success. It seems unlikely that a misidentification of one of the ideal volumes, for the dodecahedron, could produce the same effect as a misidentification of a quite different ideal volume, for the icosahedron.

Thus we believe that we have found exact (and also very lengthy) expressions of the form $\sum_{k=1}^{n} D(z_k)$, with $n = 128$ and $z_k \in \mathbf{Q}(\sqrt{8\sqrt{2} - 15})$, for the cubical/octahedral volume of Table 20, and with $n = 346$ and $z_k \in \mathbf{Q}(\sqrt{-12\sqrt{5} - 31})$, for the dodecahedral/icosahedral volume of Table 21. Thanks to David Bailey's evaluations of $\zeta(2n)$, described in Section 4.2, we were able to obtain $1,800$ good digits of $2,850$ Clausen values in less than 2 hours.

5 Knots and links from Feynman diagrams

Finally, we arrive at the motivating idea for this work: values of Feynman diagrams.

14

5.1 Hyperbolic Feynman links

In [27], Andrei Davydychev and Bob Delbourgo made a fine discovery: the dilogarithms of the box diagram for particle scattering are those which give the volume of a tetrahedron in hyperbolic 3-space (or its analytic continuation).

In the 3-dimensional [28] studies of statistical physics, one-loop Feynman diagrams yield logarithms; in the 4 space-time dimensions of relativistic quantum field theory (QFT), they yield dilogarithms [29]. A connection between the dilogs of QFT and those of hyperbolic geometry was considered in [30]. The achievement of [27] is to derive a fairly simple relation between the value of any scalar box diagram, in 4 space-time dimensions, and the volume of an explicit tetrahedron in a 3-space of constant curvature. There is nothing ideal about this tetrahedron: in general it has 6 essential dihedral angles, determined by the 10 physical quantities in the problem: the 4 external masses, the 4 internal masses, and the Mandelstam variables s and t, related to the energy at which the process occurs and the angle of scatter. Already one sees a nice simplification, with 9 dimensionless ratios of physical quantities collapsing to 6 essential dihedral angles. So far, however, the question of number theory does not arise, since in the generic physical situation the kinematic quantities are real variables, and hence no algebraic number field is implied for the arguments of the dilogarithms.

Now consider the process of light-by-light scattering, where the external (photon) masses vanish and there is a common internal (electron) mass, normalized to unity. There remain the Mandelstam variables, s and t. Following work that involved comparable Clausen values [31, 32], it was observed in [1] that light-by-light scattering yields remarkable results at $s = t = n \in \{4, 5, 6, 7\}$, where the dilogs give rational multiples of the volumes of links. These links all figure in Section 4, above, where their volumes were rationally related to $Z_{|D|}$, in (23). The $n = 4$ case gives a rational multiple of Z_4, corresponding to the Whitehead link; $n = 5$ relates to Z_{15} and the link $(\sigma_1^2 \sigma_2^{-2})^3$; $n = 6$ to Z_3 and the figure-8 knot; $n = 7$ to Z_7 and 6_1^3. Moreover, a rational multiple of the volume, Z_8, of the link $9_{40}^2 := (\sigma_1^2 \sigma_2^{-1})^3$ is obtained for Mandelstam variables $s = \frac{1}{2} t = 4$.

In the course of the present work we discovered that the hyperbolic volume, Z_{20}, of the self-dual alternating platonic link of Fig. 1 corresponds to the values[13] $s = \frac{1}{2} t = 5$ for the Mandelstam variables. Perhaps not even Delbrück and Meitner[14] could have imagined that light-by-light scattering would spawn a tetrahedral hyperbolic link.

5.2 Dedekind-zeta invariants of Feynman orthoschemes

Let us try to disentangle this remarkable circumstance from its physical origin. What is the common characteristic of the Davydychev–Delbourgo (DD) hyperbolic tetrahedron at

---

[13]For a scattering above the electron-positron threshold, with $s > 4$ and $t < 0$, unitarity makes the amplitude complex. A relation to a real hyperbolic volume is obtained by analytic continuation to $t > 4$.

[14]In 1933, Max Delbrück (1906–81) and Lise Meitner (1878–1968) foresaw non-linear effects in quantum electrodynamics. See http://www.nobel.se/laureates/medicine-1969-1-bio.html for Delbrück's subsequent work on molecular genetics and sensory physiology.

those values of the physical quantities which gave the volumes of links?

In terms of (39), we define the 3-argument dilogarithm

$$
\begin{aligned}
S(\psi_1, \psi_2, \psi_3) \quad &:= \quad V(\delta + \psi_1, \delta - \psi_1) + V(\delta + \psi_3, \delta - \psi_3) \\
&+ \quad V(\tfrac{1}{2}\pi + \psi_2 - \delta, \tfrac{1}{2}\pi - \psi_2 - \delta) + V(\tfrac{1}{2}\pi - \delta, \tfrac{1}{2}\pi - \delta)
\end{aligned}
\tag{46}
$$

with an auxiliary angle $\delta \in [0, \pi/2]$ satisfying [27]

$$
\tan^2 \delta = \frac{\cos^2 \psi_2}{\cos^2 \psi_1 \cos^2 \psi_3} - \tan^2 \psi_1 \tan^2 \psi_3
\tag{47}
$$

Then the Schläfli/Lobachevsky [33, 34, 35, 36] function (46) is 4 times the volume of a bi-rectangular hyperbolic tetrahedron, with essential dihedral angles ψ_1, ψ_2, ψ_3. The edges with angles ψ_1 and ψ_3 are opposite, while that with ψ_2 is adjacent to each. The remaining 3 dihedral angles are right angles. With 3 essential angles, a bi-rectangular tetrahedron is an example of an orthoscheme [18]. With a common internal mass, and a common external mass, the DD tetrahedron comprises 4 identical orthoschemes, with (46) giving its volume.

The next step was to calculate the essential angles ψ_k that had given a rational relation to the volume of a link. In all cases we found that $\psi_k \in \{0, \pi/6, \pi/4, \pi/3\}$. The final step was clear: to compute all such instances of (46), in the hope of finding more Feynman orthoschemes that are rationally related to Dedekind zeta values. Taking account of the positivity of (47), and the symmetry $S(\psi_1, \psi_2, \psi_3) = S(\psi_3, \psi_2, \psi_1)$, there are 36 possibilities to consider, of which the physics in [1] had already shown 5 to be fruitful. We had a lively expectation of further rational relations to $Z_{|D|}$. We were thus totally delighted by the following, totally rational, finding.

> **Discovery:** All real instances of (46) with $\psi_k \in \{0, \pi/6, \pi/4, \pi/3\}$ are rational multiples of $Z_{|D|}$ with $|D| \in \{3, 4, 7, 8, 11, 15, 20, 24, 39, 84\}$. Table 22 gives the 36 empirical relations. All the relations are realized by Feynman diagrams; in the cases with $\psi_2 \neq 0$, one has merely to give the external particles a suitable common mass.

It was trivial to decide which value of $Z_{|D|}$ to try in each of the 36 cases: one has only to examine the square root of (47) to determine D. Had we been less result-oriented we might have taken time out to recast[15] each of the 36 searches in terms of 4 complex arguments of Bloch–Wigner dilogarithms for the 4 ideal parts of (46), and then used algebra [17, 19] to determine, in advance, whether a rational (but unspecified!) number would result from dividing the volume by $Z_{|D|}$. We were content with the faster process of division, which gives the concrete result. Throughout this work, the issue is not the existence of rationals, but their values. The rational numbers of Table 22 in the cases

---

[15]There is nothing complex, or ideal, in the physical problem that led to our discoveries: integration over real Feynman parameters yields the volume of a tetrahedron, none of whose vertices are at infinity.

with $-D \geq 7$ are at least as hard to derive as those in (26–30,37). For $D = -39$, we found that

$$24\mathrm{Cl}_2(\theta_{13,3}) - 15\mathrm{Cl}_2(2\theta_{13,3}) + \mathrm{Cl}_2(6\theta_{13,3}) = \tfrac{1}{6}Z_{39} \tag{48}$$

with $\theta_{13,3} := 2\arctan\sqrt{13/3}$. For $D = -84$, we found that

$$60\mathrm{Cl}_2(\theta_{7,3}) - 36\mathrm{Cl}_2(2\theta_{7,3}) - 4\mathrm{Cl}_2(3\theta_{7,3}) + 3\mathrm{Cl}_2(4\theta_{7,3}) + 2\mathrm{Cl}_2(6\theta_{7,3}) = \tfrac{1}{6}Z_{84} \tag{49}$$

with $\theta_{7,3} := 2\arctan\sqrt{7/3}$. These are our 7th and 8th unprovens, courtesy of Feynman.

5.3 Two of Feynman's links are missing

The rationale for the underlinings in (19) should now be clear: it was these 10 imaginary-quadratic fields that had been distinguished by the Feynman orthoschemes of Table 22, which initiated our studies. For 4 of these 10 fields, the census gave links; for 2 of the remaining 6, the work in [1] gave links; for 2 of the remaining 4, the alternating platonic link of Fig. 1 and the non-alternating daisy-chain link of Fig. 2 supplied answers; that left us with the $D = -39$ and $D = -84$ links still missing.

It may be imagined that we spent much time looking for Feynman's two missing links. We find it significant that, in all our exploration, SnapPea never detected a quadratic field beyond those we have reported, with $-D \in \{3, 4, 7, 8, 11, 15, 20, 24\}$. One could, if one was minded, synthesize cusped manifolds with gluing conditions that are satisfied in other quadratic fields, and then assert the existence of links whose complements in S^3 are isometric to these manifolds. Our aim was more concrete, and perhaps more old-fashioned. Just as the basic ingredients of Table 22 would have been immediately intelligible to their originators[16] Nikolai Ivanovich Lobachevsky and Thomas Clausen, so would those of Figs. 1 and 2 have been to[17] James Clerk Maxwell and Peter Guthrie Tait.

It was, therefore, very satisfying to progress to $D = -24$, at 48 crossings, and not to encounter any quadratic SnapPea triangulation beyond those we had learnt to expect from Feynman, Davydychev and Delbourgo. By the same token, it was frustrating not to discover two more Feynman links, with volumes rationally related to Z_{39} and Z_{84}.

We hope that others will be motivated to search. Table 19 indicates the challenge. The self-dual platonic link of Fig. 1 entails 24 crossings, 10 components, and a volume $Z_{20} = \mathrm{vol}(24^{10}_{\mathrm{tet}}) \approx 50.447$; the daisy-chain link of Fig. 2 entails 48 crossings and 24 components, to reach $Z_{24} = V_{24} - V_8 \approx 62.186$. The reader is left to imagine what might be entailed by $Z_{39} \approx 165.575$ and $Z_{84} \approx 404.736$.

In any case, one now knows that Feynman orthoschemes[18] at Mandelstam variables $s = 3t = 13$ and $s = \tfrac{3}{2}t = 7$ are rationally related to (23) at $D = -39$ and $D = -84$,

---

[16]The geometry of Lobachevsky (1792–1856) gives a model for the Universe that accords with data. Clausen (1801–85) was an astronomer, described by Gauss (1777–1855) as a man of outstanding talents.

[17]Maxwell (1831–79) and Tait (1831–1901) were schoolfriends in Edinburgh. Maxwell later formulated electromagnetic field theory and encouraged Tait's search for a connection between knots and physics.

[18]The Feynman diagram evaluates to the volume of orthoscheme (46) divided by a square root.

with coefficients in (48,49) that are as easy to measure, and as hard to prove, as those which are reified in Figs. 1 and 2. It is hard to believe that the 2 missing links will be less beautiful than the 8 which we have already related to Feynman orthoschemes.

5.4 Dedekind zeta values from 10-crossing Feynman knots

We found that 7 of the 84 knots with less than 10 crossings have rational Dedekind-zeta invariants. The 6 distinct values of (1) are

$$Z_3 = 1 \times \mathrm{vol}(4_1) \tag{50}$$
$$Z_{23,3} = \tfrac{1}{3} \times \mathrm{vol}(5_2) = \tfrac{1}{10} \times \mathrm{vol}(9_{49}) \tag{51}$$
$$Z_{44,3} = \tfrac{1}{3} \times \mathrm{vol}(9_{48}) \tag{52}$$
$$Z_{59,3} = 1 \times \mathrm{vol}(7_4) \tag{53}$$
$$Z_{76,3} = 1 \times \mathrm{vol}(9_{35}) \tag{54}$$
$$Z_{448,4} = \tfrac{1}{6} \times \mathrm{vol}(8_{18}) \tag{55}$$

where the subscripts of $Z_{|D|,n}$ identify the (negated) discriminant and degree of the number field, and we omit the latter in the quadratic case. Two further knots, 8_{21} and 9_{28}, have invariant trace fields in Table 18. From these subfields of joins, one may extract

$$Z_7 = 4 \times \mathrm{vol}(8_{21}) - \tfrac{4}{3} \times \mathrm{vol}(8_{18}) \tag{56}$$
$$Z_{507,4} = \tfrac{2}{5} \times \mathrm{vol}(9_{28}) - 1 \times \mathrm{vol}(4_1) \tag{57}$$

We now report on two very special knots at 10 crossings. Work begun by Dirk Kreimer [37, 38, 39], and extended in collaborations with Broadhurst, Delbourgo and Gracey [11, 12, 13, 14], has established a rich connection between multiple zeta values [40, 41, 42, 43] and positive knots, forged by multi-loop Feynman diagrams in quantum field theory. A positive knot is one with a minimal braid word that entails exclusively positive powers of the generators of the braid group [44]. There is an important feature to note: no positive knot with less than 10 crossings is hyperbolic. The 5 positive knots with less than 10 crossings are the $(3,2)$, $(5,2)$, $(7,2)$, $(4,3)$ and $(9,2)$ torus[19] knots, with 3, 5, 7, 8 and 9 crossings, corresponding to $\zeta(3)$, $\zeta(5)$, $\zeta(7)$, $\zeta(5,3)$ and $\zeta(9)$, where $\zeta(r,s) := \sum_{j>k>0} j^{-r}k^{-s}$ is a multiple zeta value (MZV) of depth 2 and weight $r+s$, with $\zeta(5,3)$ being the sole irreducible MZV below weight 10.

The first 2 hyperbolic Feynman knots are $10_{139} := \sigma_1 \sigma_2^3 \sigma_1^3 \sigma_2^3$ and $10_{152} := \sigma_1^2 \sigma_2^2 \sigma_1^3 \sigma_2^3$, with volumes

$$\mathrm{vol}(10_{139}) = 4.851170757332737567058327052115312478845283027 7699\ldots \tag{58}$$
$$\mathrm{vol}(10_{152}) = 8.536065347205608603144181920549325994964991396 9140\ldots \tag{59}$$

that are rather modest, compared with most of the other 162 hyperbolic 10-crossing knots.

---

[19]Non-hyperbolic knots are torus or satellite knots, with the latter beginning at 13 crossings.

We do not know how many of the 164 hyperbolic 10-crossing knots enjoy single-complex-place invariant trace fields, though we may estimate the fraction from 3 previous results. We found rational relations for $998/11031 \approx 9\%$ of the closed census manifolds, for $312/4929 \approx 6\%$ of the cusped census manifolds, and for $7/79 \approx 9\%$ of the hyperbolic knots with less than 10 crossings. It thus seems unlikely that more than 10% of 10-crossing knots have rational Dedekind invariants. Had we selected a pair at random, the odds on both having single-complex-place invariant trace fields would be of order $100:1$ against. Yet the volumes (58,59) were not chosen at random; they come from the unique pair of positive hyperbolic 10-crossing knots.

It is, therefore, both notable and gratifying that the Feynman knots 10_{139} and 10_{152} both yield simple rational Dedekind-zeta invariants, namely 1 and $1/2$, corresponding to the Dedekind zeta values

$$\zeta_{K_{139}}(2) = 1 \times \frac{(2\pi)^6 \text{vol}(10_{139})}{12 \times 688^{3/2}} \tag{60}$$

$$\zeta_{K_{152}}(2) = \frac{1}{2} \times \frac{(2\pi)^8 \text{vol}(10_{152})}{12 \times 8647^{3/2}} \tag{61}$$

for the single-complex-place quartic and quintic fields

$$K_{139} := x^4 - 2x - 1 \tag{62}$$

$$K_{152} := x^5 - 3x^3 - 2x^2 + 2x + 1 \tag{63}$$

where K_{139} is also the invariant trace field of the link 8_2^2, with the same volume as 10_{139}.

There is an important distinction between the 2 hyperbolic Feynman knots at 10 crossings and the sole hyperbolic Feynman knot at 11 crossings, associated with the irreducible [40, 41] triple sum $\zeta(3,5,3) = \sum_{j>k>l>0} j^{-3}k^{-5}l^{-3}$. At 10 crossings it has not yet been possible to identify the generalized polylogarithms of weight 10 in the 7-loop[20] Feynman diagrams [11] that skein to gives these knots. We know that each involves more than MZVs, since $\zeta(7,3)$ is accounted for by the $(5,3)$ torus knot, 10_{124}

Plans are afoot to compute, to high precision, the numbers associated by QFT to 10_{139} and 10_{152}. Discussion with Andrei Davydychev and Dirk Kreimer suggests that it may be possible to extract values from high-order ε-expansions of multi-loop dressings of 2-loop skeletons in $4 - 2\varepsilon$ spacetime dimensions, with dressings deliberately chosen to frustrate reduction to MZVs. If that project bears fruit, there will be scope for PSLQ searches, beyond what is possible with current 10-digit data from 7-loop diagrams.

It is believed that promising targets for such integer-relation searches might be provided by volumes of polytopes in hyperbolic spaces of odd dimensions substantially greater than 3, and perhaps as large as 13, which may present a computational challenge to geometers as great as that confronting quantum field theorists at 7 loops. However, it will do no harm to include in PSLQ searches the easily computed weight-10 quintic Dedekind zeta value (61), from 3 dimensions, which would correspond to the less likely hypothesis that the associated geometry is simpler than appears from the 7-loop physics.

---

[20]The loop number, L, is the number of 4-dimensional integrations over internal momenta; the crossing number does not exceed $2L - 3$. Numerical analysis of 28-dimensional integrals is rather taxing.

We noted that at 9 crossings the 3 knots with rational Dedekind-zeta invariants comprise the $3, 3, 3$ pretzel knot 9_{35}, in (54), and a pair of non-alternating knots, namely 9_{48} and 9_{49}, in (51,52). Accordingly, we sought for further single-complex-place fields among the 10-crossing pretzels, namely $10_{46} := 5, 3, 2$ and $10_{61} := 4, 3, 3$, and the remaining non-alternating hyperbolic 10-crossing knots, namely $\{10_n | 165 \geq n \geq 125; n \neq 139; n \neq 152\}$. From these 41 knots we obtained only 2 results:

$$Z_{31,3} = \tfrac{1}{8} \times \mathrm{vol}(10_{157}) = \tfrac{1}{3} \times \mathrm{vol}(7_1^2) \tag{64}$$
$$Z_{29963,5} = 4 \times \mathrm{vol}(10_{153}) \tag{65}$$

providing a measure of how privileged is the Feynman [11, 14] pair, 10_{139} and 10_{152}. There was one join, already found in (57) at 9 crossings, with

$$Z_3 + Z_{507,4} = \tfrac{1}{2} \times \mathrm{vol}(10_{155}) = \tfrac{2}{5} \times \mathrm{vol}(9_{28}) \tag{66}$$

We note that the first example of degenerate volumes, provided by

$$\mathrm{vol}(10_{132}) = \mathrm{vol}(9_{42}) \tag{67}$$

does not yield a rational invariant, since the quintic invariant trace fields are generated by $x^5 - x^4 - 2x^2 + 2x - 1$, with 2 complex places.

We also remark on the alternating knot 10_{123}. Like 9_{41}, it has a two-complex-place invariant trace field, generated by a root of $x^4 - x^3 + x^2 - x + 1$. Thus its volume is provably related to Clausen values at multiples of $\pi/5$. Interestingly, both knots have volumes that are rationally related to instances of the orthoscheme (46), with

$$S\left(\tfrac{2}{5}\pi, \tfrac{1}{10}\pi, \tfrac{1}{5}\pi\right) = \tfrac{1}{10} \times \mathrm{vol}(9_{41}) = \mathrm{Cl}_2\left(\tfrac{2}{5}\pi\right) + \tfrac{1}{3}\mathrm{Cl}_2\left(\tfrac{4}{5}\pi\right) \tag{68}$$
$$S\left(\tfrac{3}{10}\pi, \tfrac{1}{5}\pi, \tfrac{1}{10}\pi\right) = \tfrac{1}{10} \times \mathrm{vol}(10_{123}) = \tfrac{2}{3}\mathrm{Cl}_2\left(\tfrac{2}{5}\pi\right) + \tfrac{1}{3}\mathrm{Cl}_2\left(\tfrac{4}{5}\pi\right) \tag{69}$$

The corresponding relations between Clausen values are straightforward to derive, and hence quite unlike those with $-D \geq 7$ in Table 22, which involve the 8 dramatic switches between number fields recorded in (26–30,37,48,49).

5.5 Dedekind zeta values from 12-crossing Feynman knots

At 12 crossings, corresponding to 8 loops in QFT, Broadhurst and Kreimer [14] found that 7 of the 2,176 hyperbolic knots are positive. We found that 3 of these have rational Dedekind-zeta invariants, with

$$Z_{23,3} = \tfrac{1}{3} \times \mathrm{vol}(\sigma_1 \sigma_2^3 \sigma_1 \sigma_2^7) \tag{70}$$
$$Z_{848,4} = 1 \times \mathrm{vol}(\sigma_1 \sigma_2^5 \sigma_1 \sigma_2^5) \tag{71}$$
$$Z_{2068,4} = 2 \times \mathrm{vol}(\sigma_1^3 \sigma_2^3 \sigma_1^3 \sigma_2^3) \tag{72}$$

The first two are those identified as Feynman knots in [13, 14]. Again, we find it uncanny that, with odds of at least $100 : 1$ against, both Feynman knots proved to have single-complex-place invariant trace fields. It is clear that the Dedekind single-complex-place

criterion and the Feynman positivity criterion are strongly related. The origin of this association is, however, quite unclear to us.

Most notable is the result (70) for the 12-crossing positive knot with braid word $\sigma_1\sigma_2^3\sigma_1\sigma_2^7$, which is associated [13] with the irreducible MZV $\zeta(9,3)$ in QFT. It has a rather small, and very special, volume:

$$\text{vol}(\sigma_1\sigma_2^3\sigma_1\sigma_2^7) = \text{vol}(5_2) = \tfrac{3}{10} \times \text{vol}(9_{49}) = \tfrac{3}{7} \times \text{vol}(7_2^2) = 3Z_{23,3} \approx 2.828122 \qquad (73)$$

which is precisely 3 times the volume of the closed Weeks manifold, m003$(-3, 1)$, conjectured to be the smallest of all hyperbolic manifolds. The knot $\sigma_1\sigma_2^3\sigma_1\sigma_2^7$ is the first in the sequence of hyperbolic Feynman knots [14] $F_{2n} := \sigma_1\sigma_2^3\sigma_1\sigma_2^{2n-5}$, with $2n \geq 12$ crossings, associated with $\zeta(2n-3,3)$ in Feynman diagrams with $n + 2 \geq 8$ loops.

We found that the equality of the volumes of F_{12} and 5_2 generalizes to

$$\text{vol}(\sigma_1\sigma_2^3\sigma_1\sigma_2^{2n-5}) = \text{vol}(\sigma_1\sigma_2^3\sigma_1\sigma_2^{11-2n}) \qquad (74)$$

where the knot on the r.h.s. is formally obtained by $n \to 8 - n$ and has no more than $2n - 6$ crossings. For $2n \geq 12$ we also found that

$$\text{vol}(F_{12}) \leq \text{vol}(F_{2n}) \leq \text{vol}(9_{60}^2) = \tfrac{1}{2}Z_7 \approx 5.333489 \qquad (75)$$

where Z_7 is the pivot of (26), which is the first of the non-trivial Clausen relations from 1-loop box diagrams. At large n, the behaviour was measured to be

$$\text{vol}(F_{2n}) = \tfrac{1}{2}Z_7 - \frac{C}{(\tfrac{1}{4}n - 1)^2} + O(1/n^4) \qquad (76)$$

with $C \approx 0.8160$, found from 12-digit SnapPea results, with up to 500 crossings.

The asymptote suggested that the manifolds complementary to the series F_{2n} of Feynman knots might be isometric to a series of Dehn fillings of a manifold with volume $\tfrac{1}{2}Z_7$. The `drill` command of Snap suggested the manifold s785, which we found to be isometric to the complement of the link 9_{60}^2. Performing the surgeries $(-2, 1) \ldots (-21, 1)$ on its second cusp, we obtained 20 manifolds and asked SnapPea to compare them with the manifolds complementary to the Feynman knots F_{2n}, with crossing numbers from 12 to 50. The result was isometry, in all 20 cases. It was then possible to compute 64 good digits of

$$C = 0.8160162119959694990691941006445603982758744790599736680521553757\ldots \qquad (77)$$

from 20 high-precision Snap triangulations of s785$(,)(4-n, 1)$, with $n = O(10^3)$. It would be interesting to obtain analytical results for asymptotic changes [45] in volume, such as that given by (77).

Now one sees the origin of the invariance (74) of volumes, under the transformation $n \to 8 - n$. This merely flips a sign of the Dehn surgery on the torus [46] curve $(4 - n, 1)$. The fixed point, at $n = 4$, is the non-hyperbolic longitudinal surgery $(0, 1)$, corresponding to the $(4, 3)$ torus knot, $F_8 := (\sigma_1\sigma_2^3)^2 \sim (\sigma_1\sigma_2)^4 = 8_{19}$, which is the first 3-braid

Feynman knot, found at 6 loops [11] in QFT, where it signals the appearance of the first irreducible [40, 41] MZV, $\zeta(5,3)$, in the counterterms of ϕ^4-theory. At 7 loops, with $n = 5$, the surgery $(-1, 1)$ is likewise non-hyperbolic, corresponding to the $(5, 3)$ torus knot $F_{10} := \sigma_1 \sigma_2^3 \sigma_1 \sigma_2^5 \sim (\sigma_1 \sigma_2)^5 = 10_{124}$, associated with $\zeta(7,3)$. Only at 12 crossings, and hence 8 loops, does this series of Feynman knots start to be hyperbolic. One thus expects to find a rather special volume at 12 crossings, as is indeed seen in (73).

5.6   Dedekind zeta values from maximally symmetric knots

Jim Hoste, Morwen Thistlethwaite and Jeff Weeks (hereafter HTW) have recently completed an impressive symmetry analysis [15] of all 1,701,936 prime knots with up to 16 crossings. From the University of Tennessee at Knoxville, we obtained files[21] that identify highly symmetric alternating and non-alternating knots at crossing numbers from 11 to 16. Before analyzing the most symmetric of these, we comment on the situation up to 10 crossings, in territory charted by Dale Rolfsen [26] and predecessors.

Table 23 gives the hyperbolic alternating and non-alternating[22] knots of maximal symmetry at crossing numbers from 4 to 10, together with the symmetry groups, invariant trace fields, signatures and discriminants of their complementary manifolds. Where the field has a single complex place (i.e. signature $[n - 2, 1]$ at degree n) we give the rational Dedekind-zeta invariant, a/b. Table 24 shows our remaining finds of Dedekind-zeta invariants, for knots up to 10 crossings. The latter are likely to be complete up to 9 crossings; at 10 crossings we analyzed all non-alternating knots, but only about 20% of the alternating knots.

Some comments are in order.

1. Up to 9 crossings, maximal symmetry is a good – yet far from infallible – diagnostic of a single-complex-place field.

2. The maximally symmetric knots designated by Rolfsen [26] as 6_3, 7_7, 8_{21}, 9_{40} and 10_{123} have invariant trace fields with more than one complex place.

3. In (56) it is shown that the volume of 8_{21} reduces to a pair of Dedekind zeta values.

4. In (69) it is shown that the volume of 10_{123} reduces to that of a simple orthoscheme.

5. Only one Dedekind-zeta knot, namely 9_{49}, escapes the sieve of maximal symmetry up to 9 crossings. Moreover, (51) shows that it yields a Dedekind zeta value already encountered at fewer crossings.

6. At 10 crossings, we found 3 non-alternating Dedekind-zeta knots with less than maximal symmetry: the Feynman [11, 14] pair, 10_{139} and 10_{152}, with the modest symmetries D_2 and Z_2, and 10_{153}, which SnapPea declared to be devoid of symmetry.

---

[21]http://www.math.utk.edu/~morwen/knotscape.html
[22]Below 8 crossings, all hyperbolic knots are alternating.

In the light of the above, we were prepared for a dwindling yield from maximal symmetry, above 10 crossings. The harvest proved to be even more meagre than we anticipated. Table 25 shows that *none* of the 11 maximally – and visibly [15] – symmetric alternating knots from 11 to 16 crossings has a single-complex-place invariant trace field. From the 10 maximally – and covertly [15] – symmetric non-alternating knots, we obtained 4 single-complex-place fields, yet only one of these entailed a new Dedekind zeta value, namely

$$Z_{643,4} = \tfrac{1}{5} \times \mathrm{vol}(\mathrm{n}14.13191) \tag{78}$$

while those in

$$\begin{aligned}
Z_{44,3} &= \tfrac{1}{4} \times \mathrm{vol}(\mathrm{n}12.642) & (79)\\
Z_{448,4} &= \tfrac{1}{10} \times \mathrm{vol}(\mathrm{n}15.112310) & (80)\\
Z_{31,3} &= \tfrac{1}{15} \times \mathrm{vol}(\mathrm{n}16.1007813) & (81)
\end{aligned}$$

had already been obtained in (52,55,64). The last of these duplicates merits further comment.

There are more [15] than a million non-alternating hyperbolic 16-crossing knots. Amid this plethora, HTW identified the 1,007,813th (in their lexicographic ordering of Dowker codes) as uniquely maximally symmetric. It enjoys the 18-fold dihedral symmetry group D_9 of the nonagon, exquisitely disguised in any 16-crossing projection. If the reader has access to SnapPea, s/he should certainly not miss the opportunity to click in a depiction of the non-alternating knot in Fig. 7 of the highly readable article[23] by HTW. Then the power of Jeff Weeks' topological engine [21] becomes apparent, when its symmetry analyzer announces D_9. Morwen Thistlethwaite's website[24] renders this more visible, by resort to a 5-braid presentation.

Intuition told us to expect a Dedekind zeta value from the HTW knot with symmetry group D_9. In this respect, we were not disappointed: the volume of the knot is $15\,Z_{31,3}$, giving a Dedekind-zeta invariant $a/b = 1/15$ that is smaller than any we had previously encountered. We allayed the disappointment, at having already encountered $Z_{31,3}$, by the following *ex post facto* considerations. The D_9 knot is so special that it merits a simple invariant trace field. The quadratic field $\mathbf{Q}(\sqrt{-3})$ was taken by the figure-8 knot, in (50). The cubic field with $D = -23$ had already been engaged by Feynman, at 12 crossings, in (73). The next cubic discriminant, $D = -31$, provides an eminently suitable resting place for the Hoste–Thistlethwaite–Weeks D_9 knot. Colleagues engaged on commensurability [7] analyses may now investigate the wondrously long chain

$$\begin{aligned}
Z_{31,3} &= \tfrac{1}{15} \times \mathrm{vol}(\mathrm{n}16.1007813) & (82)\\
&= \tfrac{1}{8} \times \mathrm{vol}(10_{157}) & (83)\\
&= \tfrac{1}{4} \times \mathrm{vol}(\mathrm{v}3183) & (84)\\
&= \tfrac{1}{3} \times \mathrm{vol}(7_1^2) & (85)\\
&= \tfrac{1}{2} \times \mathrm{vol}(\mathrm{m}034) & (86)
\end{aligned}$$

---

[23]http://www.pitzer.edu/~jhoste also gives access to [15].
[24]http://www.math.utk.edu/~morwen/d9.html

$$= \quad 1 \quad \times \text{vol}(\text{m007}(+4, 1)) \tag{87}$$
$$= \quad \tfrac{2}{3} \quad \times \text{vol}(\text{m149}(+1, 2)) \tag{88}$$
$$= \quad \tfrac{2}{7} \quad \times \text{vol}(\text{v1963}) \tag{89}$$

of distinct rational Dedekind-zeta invariants from a common invariant trace field. The last 6 invariants cover 43 census manifolds. The volumes of the D_9 knot and 10_{157} are $30\,D(z)$ and $16\,D(z)$, where $z^3 = 1 - z$, with $\Im z > 0$, and $D(z) = \tfrac{1}{2}Z_{31,3}$ is the volume of any one of the 4 ideal tetrahedra that triangulate m034. Here, as in the Feynman case (73), the Dedekind zeta value collapses to a rational multiple of a single Bloch–Wigner dilogarithm.

5.7 Dedekind zeta value from an 18-crossing Feynman knot

It was observed that the positivity criterion of [11, 13, 14] was more fertile than maximal symmetry, at 10 and 12 crossings. We expect further sequences of positive knots whose first hyperbolic instances yield Dedekind zeta values at high crossing numbers. From QFT we inferred a source of such a sequence, namely the 3-parameter family of even-crossing positive 3-braids [14]
$$R_{k,m,n} := \sigma_1 \sigma_2^{2k} \sigma_1 \sigma_2^{2m} \sigma_1 \sigma_2^{2n+1} \tag{90}$$
We knew from [14] that $R_{2,2,1}$ is the 14-crossing torus knot $(7, 3)$. Dirk Kreimer helped us show that $R_{3,2,1}$ is the 16-crossing torus knot $(8, 3)$. But $R_{4,2,1}$ cannot be a torus knot, since 9 and 3 are not coprime. The 18-crossing hyperbolic volume is intriguingly small:

$$\text{vol}(R_{4,2,1}) = 3.4742477613127422960290085536119319187978177080 5621 \dots \tag{91}$$

Table 13b immediately identified the invariant trace field as a single-complex-place sextic, with $D = -753079$. Table 6 then gave $x^6 - x^5 - 3x^4 - x^3 + 2x^2 + 2x - 1$ as the generating polynomial. SnapPea confirmed isometry of the complement of $R_{4,2,1}$ with manifold m082. The corresponding rational Dedekind-zeta invariant, $a/b = 26$, in

$$Z_{753079,6} = 26 \times \text{vol}(R_{4,2,1}) \tag{92}$$

is larger than we had found for any graphically generated knot, and is 390 times that for the D_9 knot, in (82). For the 5th time of asking, a positive Feynman knot gives a Dedekind zeta value. The odds on this being accidental are at least $10^5 : 1$ against.

Lest such a connection between knots, numbers and Feynman diagrams be thought exceptional, we recall that at 8 crossings QFT demanded [11] a positive 3-braid knot and an irreducible depth-2 MZV, which were duly forthcoming, in the shape of 8_{19} and $\zeta(5, 3)$. At 11 crossings, the demands were similarly imperious: a positive 4-braid knot and an irreducible depth-3 MZV, satisfied by the uniqueness [11] of $\sigma_1 \sigma_2^3 \sigma_3^2 \sigma_1^2 \sigma_2^2 \sigma_3$ and the irreducibility [40] of $\zeta(3, 5, 3)$. At 12 crossings, QFT seemed, at first, to require something perverse: an arbitrary choice between an irreducible depth-4 MZV and an irreducible depth-2 alternating [40] Euler sum. Mathematics accommodated, via the remarkable discovery [13, 14, 40] that one is reducible to the other. Compared with these past findings, a new Dedekind zeta value, at 18 crossings, is small fry to the maw of natural philosophy.

It took 50 years to discover that the renormalization of QFT is governed by a Hopf algebra [47], richer than that of noncommutative geometry [48], and readily automated [49]. This offers the prospect of elucidating the existence of analytically non-trivial 4-term relations [50, 51] in realistic (i.e. 4-dimensional) QFT. Hopefully, our latest addition of a Dedekind-zeta connection, to the melting-pot of knot/number/field theory [52], may also be illuminated by the joint efforts of physicists and mathematicians who are responsive to empirical data.

6 Conclusions and prospects

Perhaps more than in any other piece of research which either author has undertaken, this work has been vitally enabled by the internet. It provided us with the opportunity to blend number theory, topology, geometry, analysis, physics and computer science, in a global empirical mixing bowl, thanks to:

- ready access to significant data at Bordeaux, Claremont CA, Florham Park NJ, Knoxville TN, Melbourne, Minneapolis MN, as detailed in footnotes;

- the ability to run high-level packages, such as Maple, Pari and Reduce, on whatever machine best served our purposes, irrespective of the contingencies of our personal geographic co-ordinates;

- wonderful specialized resources, downloadable as per our footnotes, namely: David Bailey's superb PSLQ and FFT routines, Oliver Goodman's port of high-precision Snap to DigitalUnix, and Al Manoharan's attractive adaptation to Windows95 of Jeff Weeks' amazing SnapPea program, all supported by generous email advice;

- access to powerful computers in England, Newfoundland[25] and Vancouver, yielding high-precision results such as those in (7) and (77), and the 1800-digit hyperbolic volumes of Tables 20 and 21, achieved by dedicated multiple-precision [22] code, after exploratory work enabled by the above.

The facility with which we were able to plug into all these valuable resources advertises how rich the opportunities for empirical mathematics are becoming. The tools came together to offer more patterns than we had dared to hope for. Enterprises such as we have limned promise to be more and more a part of mathematical and physical research in the next few decades.

That said, many of the results which we have exhibited remain tantalizingly far from proof, let alone understanding. Here we repeat 4 of many remaining puzzles:

- How might one begin to derive relations such as (16), between dilogarithms with arguments in radically different number fields?

---

[25]http://www.cecm.sfu.ca/~jborwein/PUP_report_March15/report.html

- Why do 1-loop Feynman diagrams, at very specific values of the Mandelstam variables, generate even more relations than we were able to reify by quadratic links?

- Why do Feynman diagrams, with 7, 8 and 11 loops, lead to 5 Dedekind-zeta knots, at 10, 12 and 18 crossings, with odds of a chance association being at least $10^5 : 1$ against?

- Can the mere dilogarithms of 3-dimensional hyperbolic geometric tell us anything about the unidentified 10th-order polylogarithms of 7-loop quantum field theory?

When faced by such visible expansion of one's lack of wisdom, it is probably best to concentrate on that which is easiest to state. Hence we conclude with a rewriting of the simplest unproven relation (16) in terms of the Dirichlet series (20). From light-by-light scattering at $s = t = 7$, and – just as mysteriously – from the hyperbolic volume of the link 6_1^3, we infer that

$$
\sum_{n>0} \left\{ 3 \left(-\frac{3}{4} + \frac{\sqrt{-7}}{4} \right)^n - 3 \left(-\frac{3}{4} + \frac{\sqrt{-7}}{4} \right)^{2n} + \left(-\frac{3}{4} + \frac{\sqrt{-7}}{4} \right)^{3n} \right\} \frac{1}{n^2}
$$
$$
= 13\, \zeta(2) - 6\, \pi \arctan \sqrt{7} + \frac{7\sqrt{-7}}{4} \sum_{n>0} \left(\frac{n}{7} \right) \frac{1}{n^2} \tag{93}
$$

The real part of this empirical and indubitable equality is easily proven; in its imaginary part, with the Jacobi symbol $\left(\frac{n}{7} \right)$, resides a flinty kernel which is – to us at least – intractable. A proof of (93) and the other quadratic identities would be most welcome.

Acknowledgments

References

[1] D.J. Broadhurst, Solving differential equations for three-loop diagrams: relation to hyperbolic geometry and knot theory,
http://xxx.lanl.gov/abs/hep-th/9806174

[2] D. Zagier, Hyperbolic manifolds and special values of Dedekind zeta-functions, *Invent. Math.*, **83** (1986) 285–301.

[3] D. Zagier, The remarkable dilogarithm, *J. Math. Phys. Sci.*, **22** (1988) 131–145.

[4] D. Zagier, Polylogarithms, Dedekind zeta functions and the algebraic K-theory of fields, in: *Arithmetic algebraic geometry (Texel, 1989)*, Progr. Math. **89**, Birkhäuser, Boston, 1991, pp. 391–430.

[5] H. Cohen, *A course in computational algebraic number theory*, Graduate Texts in Mathematics **138**, Springer-Verlag, 1993.

[6] M. Pohst and H. Zassenhaus, *Algorithmic algebraic number theory*, Cambridge University Press, 1989.

[7] D. Coulson, O.A. Goodman, C.D. Hodgson and W.D. Neumann, Computing arithmetic invariants of 3-manifolds, preprint.

[8] C. Adams, M.V. Hildebrand and J.R Weeks, Hyperbolic invariants of knots and links, *Trans. AMS*, **326** (1991) 1–56.

[9] M. Hildebrand and J. Weeks, A computer generated census of cusped hyperbolic 3-manifolds, in: *Computers and Mathematics*, eds. E. Kaltofen and S. Watt, Springer-Verlag, 1989, pp. 53–59.

[10] P.J. Callahan, M.V. Hildebrand and J.R. Weeks, A census of cusped hyperbolic 3-manifolds, *Math. Comp.*, in press.

[11] D.J. Broadhurst and D. Kreimer, Knots and numbers in ϕ^4-theory to 7 loops and beyond, *Int. J. Mod. Phys.*, **C6** (1995) 519–524.

[12] D.J. Broadhurst, R. Delbourgo and D. Kreimer, Unknotting the polarized vacuum of quenched QED, *Phys. Lett.*, **B366** (1996) 421–428.

[13] D.J. Broadhurst, J.A. Gracey and D. Kreimer, Beyond the triangle and uniqueness relations: non-zeta counterterms at large N from positive knots, *Z. Phys.*, **C75** (1997) 559–574.

[14] D.J. Broadhurst and D. Kreimer, Association of multiple zeta values with positive knots via Feynman diagrams up to 9 loops, *Phys. Lett.*, **B393** (1997) 403–412.

[15] J. Hoste, M. Thistlethwaite and J. Weeks, The first 1,701,936 knots, *Math. Intelligencer*, **20** (1988) 33–48.

[16] J. Browkin, K-theory, cyclotomic equations and Clausen's function, in: *Structural Properties of Polylogarithms*, ed. L. Lewin, Amer. Math. Soc., 1991, pp. 233–274.

[17] S. Bloch, Function theory of polylogarithms, in: *Structural Properties of Polylogarithms*, ed. L. Lewin, Amer. Math. Soc., 1991, pp. 275–286.

[18] R. Kellerhals, The dilogarithm and volumes of hyperbolic polytopes, in: *Structural Properties of Polylogarithms*, ed. L. Lewin, Amer. Math. Soc., 1991, pp. 301–336.

[19] D. Zagier, Special values and functional equations of polylogarithms, in: *Structural Properties of Polylogarithms*, ed. L. Lewin, Amer. Math. Soc., 1991, pp. 377–390.

[20] W.D. Neumann and J. Yang, Bloch invariants of hyperbolic 3-manifolds, *Duke Math. J.*, in press.

[21] J. Weeks, SnapPea in three-dimensional topology, *Topology Atlas*, **2** (1996) 24.

[22] D.H. Bailey, Multiprecision translation and execution of Fortran programs, *ACM Trans. Math. Software*, **19** (1993) 288–319.

[23] H.R.P. Ferguson, D.H. Bailey and S. Arno, Analysis of PSLQ, an integer relation finding algorithm, *Math. Comp.*, in press.

[24] B.C. Berndt, R.J. Evans and K.S. Williams, *Gauss and Jacobi sums*, CMS Series of Monographs and Advanced Texts, John Wiley, 1998.

[25] L. Lewin, *Polylogarithms and Associated Functions*, North Holland, New York, 1981.

[26] D. Rolfsen, *Knots and Links*, Publish or Perish, Berkeley, 1976.

[27] A.I. Davydychev and R. Delbourgo, A geometrical angle on Feynman integrals, *J. Math. Phys.*, **39** (1998) 4299–4334.

[28] B.G. Nickel, Evaluation of simple Feynman graphs, *J. Math. Phys.*, **19** (1978) 542–548.

[29] G. 'tHooft and M. Veltman, Scalar one-loop integrals, *Nucl. Phys.*, **B153** (1979) 365–401.

[30] N. Ortner and P. Wagner, On the evaluation of one-loop Feynman amplitudes in Euclidean quantum field theory, *Ann. Inst. H. Poincaré Phys. Theór.*, **63** (1995) 81–110.

[31] D.J. Broadhurst, Massive three-loop Feynman diagrams reducible to SC* primitives of algebras of the sixth root of unity, *Eur. Phys. J.*, in press, `http://xxx.lanl.gov/abs/hep-th/9803091`

[32] D.J. Broadhurst, A dilogarithmic three-dimensional Ising tetrahedron, *Eur. Phys. J.*, in press, `http://xxx.lanl.gov/abs/hep-th/9805025`

[33] N.I. Lobachevsky, *Imaginäre Geometrie*, Kasaner Gelehrte Schriften, 1836; Übersetzung mit Anmerkungen von H. Liebmann, Leipzig, 1904.

[34] L. Schläfli, On the multiple integral $\int \int \ldots \int dx\, dy \ldots dz$ whose limits are $p_1 = a_1 x + b_1 y + \ldots + h_1 z > 0$, $p_2 > 0, \ldots, p_n > 0$, and $x^2 + y^2 + \ldots + z^2 < 1$, *Quart. J. Math.*, **3** (1860) 54–68, 97–108, reprinted in: *Gesammelte mathematische Abhandlungen*, Band II, Birkhäuser, Basel, 1953.

[35] H.S.M. Coxeter, The functions of Lobatschefsky and Schläfli, *Quart. J. Math. Oxford*, **6** (1935) 140–144.

[36] E.B. Vinberg, Volumes of non-euclidean polyhedra (in russian), *Uspekhi Mat. Nauk*, **48** No.2 (1993) 17–46; translation in: *Russian Math. Surveys*, **48** No.2 (1993) 15–45.

[37] D. Kreimer, Knots and divergences, *Phys. Lett.* **B354** (1995) 117–124.

[38] D. Kreimer, Renormalization and knot theory, *J. Knot Theor. Ramifications*, **6** (1997) 479–581.

[39] D. Kreimer, On knots in subdivergent diagrams, *Eur. Phys. J.*, **C2** (1998) 757–767.

[40] D.J. Broadhurst, On the enumeration of irreducible k-fold Euler sums and their roles in knot theory and number theory, `http://xxx.lanl.gov/abs/hep-th/9604128`

[41] J.M. Borwein, D.M. Bradley and D.J. Broadhurst, Evaluations of k-fold Euler/Zagier sums: a compendium of results for arbitrary k, *Electronic J. Combinatorics*, **4** (1997) R5.

[42] J.M. Borwein, D.M. Bradley, D.J. Broadhurst and P. Lisonek, Special values of multidimensional polylogarithms, CECM report 98-106, May 1998.

[43] J.M. Borwein, D.M. Bradley, D.J. Broadhurst and P. Lisonek, Combinatorial aspects of multiple zeta values, *Electronic J. Combinatorics*, **5** (1998) R38.

[44] V.F.R. Jones, Hecke algebra representations of braid-groups and link polynomials, *Annals of Math.*, **126** (1987) 335–388.

[45] W.D. Neumann and D. Zagier, Volumes of hyperbolic 3-manifolds, *Topology*, **24** (1985) 307–332.

[46] C. Adams, *The Knot Book*, W.H. Freeman, New York, 1994, sect. 9.3.

[47] D. Kreimer, On the Hopf algebra structure of perturbative quantum field theories, *Adv. Theor. Math. Phys.*, **2** (1998) 303–334.

[48] A. Connes and D. Kreimer, Hopf algebras, renormalization and noncommutative geometry, *Comm. Math. Phys.*, in press, `http://xxx.lanl.gov/abs/hep-th/9608042`

[49] D.J. Broadhurst and D. Kreimer, Renormalization automated by Hopf algebra, `http://xxx.lanl.gov/abs/hep-th/9810087`

[50] D. Kreimer, Weight systems from Feynman diagrams, *J. Knot Theor. Ramifications*, **7** (1998) 61–85.

[51] D.J. Broadhurst and D. Kreimer, Feynman diagrams as a weight system: 4-loop test of a 4-term relation, *Phys. Lett.*, **B426** (1988) 339–346.

[52] D. Kreimer, *Knots and Feynman diagrams*, Cambridge Univ. Press, in press.

Table 1: Dedekind zeta values hereby related to volumes of closed manifolds

degree	2	3	4	5	6	7	8	9	10	11	12	≤ 12
number	3	11	32	38	25	19	5	3	2	1	1	140

Table 2: Quadratic fields

field	$-D$	a	b	manifold
$x^2 - x + 1$	3	2	1	m007$(+3, 1)$
$x^2 + 1$	4	2	1	m009$(+5, 1)$
$x^2 - x + 2$	7	4	1	m036$(-4, 3)$

Table 3: Cubic fields

field	$-D$	a	b	manifold
$x^3 - x^2 + 1$	23	1	1	m003$(-3, 1)$
$x^3 + x - 1$	31	1	1	m007$(+4, 1)$
$x^3 - x^2 + x + 1$	44	2	1	m006$(+3, 1)$
$x^3 + 2x - 1$	59	4	1	m004$(+6, 1)$
$x^3 - 2x - 2$	76	2	1	s784$(+1, 2)$
$x^3 - x^2 + x - 2$	83	4	1	m034$(-3, 2)$
$x^3 - x^2 + 2x + 1$	87	2	1	s784$(-1, 2)$
$x^3 - x - 2$	104	4	1	s297$(+1, 3)$
$x^3 - x^2 + 3x - 2$	107	4	1	m168$(-3, 2)$
$x^3 - x^2 - 2$	116	4	1	s881$(-1, 3)$
$x^3 - x^2 + x + 2$	139	4	1	v3106$(+3, 1)$

Table 4: Quartic fields

field	$-D$	a	b	manifold
$x^4 - x^3 + 2x - 1$	275	2	5	m016$(-4, 3)$
$x^4 - x - 1$	283	1	1	m003$(-2, 3)$
$x^4 - x^3 + x^2 + x - 1$	331	1	1	m003$(-4, 3)$
$x^4 - x^2 - 1$	400	2	5	m400$(+4, 1)$
$x^4 - 2x^3 + x^2 - 2x + 1$	448	1	1	m010$(+3, 2)$
$x^4 - x^3 - x^2 + 3x - 1$	491	1	1	m029$(-3, 2)$
$x^4 - x^3 - x^2 - x + 1$	507	1	1	m160$(-3, 2)$
$x^4 - x^3 + x^2 - x - 1$	563	1	1	m130$(+1, 4)$
$x^4 - x^3 - 2x + 1$	643	1	1	m247$(-1, 4)$
$x^4 - 2x - 1$	688	2	1	m019$(+3, 4)$
$x^4 - x^3 + 2x^2 - 1$	731	1	1	s649$(-3, 4)$
$x^4 - 2x^3 + x^2 - x - 1$	751	2	1	m081$(-4, 1)$
$x^4 - x^2 - 2x + 1$	848	2	1	m207$(-1, 3)$
$x^4 - 2x^3 + 3x^2 - 1$	976	2	1	m286$(-5, 1)$
$x^4 - x^3 + x^2 - 3x + 1$	1099	2	1	s663$(+1, 2)$
$x^4 - x^3 - 2x - 1$	1107	2	1	s928$(+4, 1)$
$x^4 - x^3 - 2x^2 - x + 1$	1156	4	1	m082$(+1, 3)$
$x^4 - x^3 + 2x^2 + x - 1$	1192	4	1	m148$(-3, 2)$
$x^4 - x^2 - 3x - 1$	1255	2	1	v3492$(+4, 3)$
$x^4 + 2x^2 - x - 1$	1371	2	1	v3489$(+2, 3)$
$x^4 - x^3 + x - 2$	1399	4	1	m293$(+2, 3)$
$x^4 - x^3 - 3x^2 + 2$	1588	8	1	m038$(+4, 1)$
$x^4 - x^3 + 3x - 1$	1732	4	1	v3187$(-4, 1)$
$x^4 - x^3 - x^2 - 2x + 1$	1791	4	1	s961$(+2, 3)$
$x^4 - x^3 - 2x^2 - 3x + 1$	1879	4	1	v2914$(+2, 3)$
$x^4 - 2x^3 + x^2 - 3x + 1$	1927	4	1	v3452$(-5, 1)$
$x^4 - 4x^2 - 2x + 2$	1968	6	1	s594$(+1, 3)$
$x^4 - x^3 - 2x^2 + 3x + 1$	2068	8	1	m389$(+3, 1)$
$x^4 - x^2 - 3x - 2$	2151	12	1	m015$(+8, 1)$
$x^4 - x^3 - 2x^2 + 3x + 2$	2319	6	1	v2944$(-5, 2)$
$x^4 - 2x^3 - x^2 + 2x - 2$	3312	12	1	v3209$(+2, 3)$
$x^4 - 5x^2 - 4$	6724	64	1	s479$(-5, 1)$

Table 5: Quintic fields

field	$-D$	a	b	manifold
$x^5 - x^3 - 2x^2 + 1$	4511	1	1	m003$(-5, 3)$
$x^5 - x^4 - x^3 + 2x^2 - x - 1$	4903	1	1	m015$(+5, 1)$
$x^5 - x^4 - x^3 + 3x^2 - 1$	5519	1	1	m016$(+3, 2)$
$x^5 - 2x^4 + x^3 + 2x^2 - 2x - 1$	5783	1	1	m016$(+2, 3)$
$x^5 - x^3 - x^2 - x + 1$	7031	1	1	m160$(-4, 1)$
$x^5 - 2x^4 + x^3 - 2x + 1$	7463	1	1	m178$(+4, 3)$
$x^5 - 3x^3 - 2x^2 + 2x + 1$	8647	2	1	m016$(+4, 1)$
$x^5 - x^4 - x^3 + x^2 - 2x + 1$	9439	1	1	v2759$(-3, 1)$
$x^5 - 2x^4 + x^2 - 2x - 1$	9759	3	1	m007$(-3, 2)$
$x^5 - x^4 - 3x^3 + 3x - 1$	10407	3	1	m023$(-4, 1)$
$x^5 - x^4 - 2x + 1$	11243	2	1	s090$(+5, 1)$
$x^5 - x^4 - 2x^3 + 3x^2 - x - 1$	11551	2	1	m223$(-1, 3)$
$x^5 + x^3 - x^2 - 3x - 1$	12447	2	1	s657$(-1, 2)$
$x^5 - 2x^2 - x + 1$	13219	2	1	s645$(+1, 3)$
$x^5 - x^4 - x^3 - x^2 - 3x + 1$	13523	2	1	v2530$(+1, 3)$
$x^5 - x^4 - 2x^3 + x + 2$	13883	2	1	v3310$(+5, 1)$
$x^5 - 2x^4 + 2x^3 - x^2 - 2x + 1$	14103	2	1	s784$(+5, 2)$
$x^5 - x^4 - 3x^3 + 3x^2 - 1$	14631	2	1	s958$(+3, 2)$
$x^5 - x^4 - 2x^3 - x^2 + 3x + 1$	14911	2	1	v2704$(-5, 1)$
$x^5 - x^4 - 2x^3 - x^2 + 2x + 2$	17348	8	1	m006$(-5, 1)$
$x^5 - 2x^4 + 4x^2 - x - 1$	22331	4	1	s884$(+2, 3)$
$x^5 - 2x^3 - x^2 - x + 1$	22424	4	1	v3246$(-2, 3)$
$x^5 - x^4 + x^2 - 3x + 1$	23103	6	1	m223$(+5, 1)$
$x^5 - x^4 + 2x^2 - 2x - 1$	23339	4	1	v3199$(+3, 1)$
$x^5 - 2x^3 - 3x^2 + x + 1$	29444	8	1	s478$(-1, 3)$
$x^5 - 2x^4 - 2x^3 + 4x^2 - x + 1$	29963	16	1	m007$(-5, 1)$
$x^5 - x^4 + 3x^2 - 6x + 2$	31684	8	1	v2381$(+3, 1)$
$x^5 - 2x^4 + 2x^3 + x^2 - 3x - 1$	34436	8	1	v2794$(-2, 3)$
$x^5 - 2x^4 + 2x^3 - 3x^2 - x + 4$	34779	9	1	v3214$(+3, 1)$
$x^5 - 2x^4 - x^3 + 2x^2 - x + 3$	38083	14	1	s437$(+1, 3)$
$x^5 - 2x^4 - x^3 + 4x^2 - 2x - 2$	58064	40	1	m141$(+2, 3)$
$x^5 - x^4 + 3x^2 - 8x + 4$	60803	28	1	m148$(+5, 1)$
$x^5 - 2x^4 - 2x^2 + 4$	70736	32	1	v2787$(-1, 3)$
$x^5 - 5x^3 - 2x^2 + 3x + 2$	79952	36	1	s594$(+3, 2)$
$x^5 - 2x^4 - 2x^3 + 4x^2 - x - 2$	107264	52	1	v3454$(-5, 1)$
$x^5 - 2x^4 - 3x^3 + x^2 + 5x + 2$	112919	88	1	m304$(+1, 3)$
$x^5 - x^4 - x^3 - 6x^2 - 7x - 2$	141791	104	1	s707$(+5, 1)$
$x^5 - 6x^3 - 5x^2 - 2x - 4$	239639	184	1	s918$(+3, 2)$

Table 6: Sextic fields

field	$-D$	a	b	manifold
$x^6 - x^5 - 2x^4 + 3x^3 - x^2 - 2x + 1$	92779	1	1	m222$(-6, 1)$
$x^6 - 2x^4 - 2x^3 + 3x + 1$	94363	1	1	m345$(+1, 2)$
$x^6 - x^5 - x^4 + 2x^3 - 2x^2 - x + 1$	104483	1	1	s648$(+1, 2)$
$x^6 - 2x^5 + x^4 - 2x^3 - x^2 + 3x - 1$	161939	2	1	s682$(+3, 1)$
$x^6 - x^5 - 2x^4 - 2x^3 + x^2 + 3x + 1$	215811	6	1	m015$(-3, 2)$
$x^6 - x^5 - 4x^4 + 4x^3 + 4x^2 - 2x - 1$	238507	7	1	m034$(+4, 1)$
$x^6 - x^5 - 2x^4 - 3x^3 + 3x^2 + 3x - 2$	365263	26	1	m004$(+3, 2)$
$x^6 - 2x^5 - 2x^4 + 6x^3 - 2x^2 - 5x + 3$	417467	13	2	v3375$(-5, 2)$
$x^6 - 2x^5 - x^4 + 5x^3 - 3x^2 - 3x + 2$	463471	16	1	m249$(+4, 1)$
$x^6 - 2x^5 - 2x^4 + 5x^3 - 3x^2 + 3x - 1$	561863	10	1	v3239$(+3, 2)$
$x^6 - 2x^5 + 6x^3 - 3x^2 - 2x + 1$	629952	18	1	s386$(+5, 2)$
$x^6 - x^5 - 3x^3 - 3x^2 + 5x - 1$	661831	16	1	v3361$(+1, 3)$
$x^6 - x^5 - x^4 + 5x^3 + x^2 - 3x - 1$	688927	14	1	v3243$(-3, 1)$
$x^6 - 4x^4 - 2x^3 + 3x^2 + 5x + 1$	709783	20	1	s952$(-4, 1)$
$x^6 - x^5 - 3x^4 - x^3 + 2x^2 + 2x - 1$	753079	26	1	m337$(-3, 1)$
$x^6 - 2x^5 - 2x^4 + 5x^3 - 2x^2 - 3x + 2$	899447	44	1	m189$(+3, 2)$
$x^6 - 2x^5 - 2x^4 + 7x^3 - x^2 - 5x + 1$	1014119	38	1	m286$(-6, 1)$
$x^6 - x^5 + 5x^3 - 4x^2 - 4x + 2$	1107052	50	1	v1315$(-4, 1)$
$x^6 - 2x^5 - 2x^4 + 4x^3 - 2x^2 - 2x + 1$	1290496	80	1	m285$(-4, 1)$
$x^6 - 2x^5 + x^4 - 3x^3 - x^2 + 5x - 2$	1494223	56	1	v3036$(+3, 2)$
$x^6 - x^5 - 3x^4 + 5x^3 + x^2 - 4x - 1$	1825672	100	1	m358$(-5, 3)$
$x^6 - 9x^3 - 10x^2 - x + 1$	2803244	236	1	m192$(-5, 2)$
$x^6 - x^5 - 4x^4 + 8x^3 + 9x^2 - 10x - 7$	4241707	296	1	v3428$(-4, 1)$
$x^6 + x^4 - 7x^3 - 2x^2 + 7x + 2$	5873596	688	1	v1858$(+6, 1)$
$x^6 - x^5 - 3x^4 + 8x^3 - 3x^2 - 7x + 1$	7792864	976	1	v2789$(-2, 3)$

Table 7: Septic fields

field	$-D$	a	b	manifold
$x^7 - x^6 - x^5 + 4x^4 - 2x^3 - 4x^2 + x + 1$	3685907	14	1	m006$(-3, 2)$
$x^7 - x^6 - 2x^5 + 5x^4 - 6x^2 + x + 1$	3998639	17	1	m004$(+5, 2)$
$x^7 - 3x^5 - 3x^4 + 4x^3 + 5x^2 - 2x - 1$	4297259	10	1	m221$(-1, 2)$
$x^7 - 2x^5 - 3x^4 - 3x^3 + 3x^2 + 4x + 1$	4795631	13	1	m032$(+5, 2)$
$x^7 - 2x^6 - x^5 + 7x^4 - 5x^3 - 5x^2 + 5x - 1$	6515927	11	1	s900$(+3, 2)$
$x^7 - 2x^6 - 3x^5 + 3x^4 + 5x^3 - x^2 - 3x + 1$	7215127	46	1	m004$(+1, 2)$
$x^7 - 2x^6 + 4x^4 - 5x^3 - 2x^2 + 4x + 1$	7557047	14	1	v2221$(-1, 3)$
$x^7 - x^6 - 5x^5 + 6x^4 + 6x^3 - 5x^2 - 2x + 1$	7729991	32	1	m038$(+1, 2)$
$x^7 - 2x^6 - 4x^5 + 6x^4 + 6x^3 - 4x^2 - 3x + 1$	9429911	20	1	s838$(-2, 3)$
$x^7 - 3x^6 - x^5 + 8x^4 - 4x^3 - 3x^2 + 5x - 2$	12558899	68	1	m070$(-3, 2)$
$x^7 - x^6 - 7x^5 + 6x^4 + 6x^3 - 11x^2 + 3x + 2$	32775179	316	1	m026$(-5, 2)$
$x^7 - 2x^6 - 4x^5 + 8x^4 + 2x^3 - 7x^2 + 5x + 1$	43210364	242	1	v3305$(-1, 2)$
$x^7 - 2x^6 - 2x^5 + 8x^4 - 2x^3 - 10x^2 + x + 3$	46692071	250	1	v2825$(-4, 1)$
$x^7 - 3x^6 - x^5 + 12x^4 - 9x^3 - 10x^2 + 8x + 1$	50052727	296	1	v2200$(-3, 2)$
$x^7 - 3x^6 - 4x^5 + 15x^4 - 11x^2 + x + 2$	58360112	788	1	m034$(+5, 2)$
$x^7 - 2x^6 - 3x^5 + x^4 + 8x^3 + 5x^2 - 6x - 3$	66467451	480	1	s523$(-6, 1)$
$x^7 - 3x^6 - 2x^5 + 11x^4 - 4x^3 - 6x^2 + 4x - 2$	75117248	616	1	v1788$(+3, 2)$
$x^7 - 2x^6 - 6x^5 + 4x^4 + 10x^3 - x^2 - 4x + 1$	81589747	828	1	m213$(-5, 2)$
$x^7 - 2x^6 - x^5 - 2x^4 + 2x^3 + 11x^2 + 2x - 2$	97569124	736	1	v3214$(+2, 3)$

Table 8: Octadic fields

field	$-D$	a	b	manifold
$x^8 - 6x^6 - 5x^5 + 7x^4$ $+ 10x^3 - x^2 - 4x - 1$	202734487	100	1	m038$(+3, 2)$
$x^8 - x^7 - 3x^6 + 7x^5 - 2x^4$ $- 8x^3 + 4x^2 + 2x - 1$	948381887	496	1	s900$(-2, 3)$
$x^8 - 2x^7 - 3x^6 + 11x^5 - 4x^4$ $- 13x^3 + 8x^2 + 5x - 2$	2095218667	2240	1	s901$(-3, 2)$
$x^8 - 3x^7 - 2x^6 + 16x^5 - 11x^4$ $- 21x^3 + 16x^2 + 12x - 1$	2401259831	1978	1	v3184$(+4, 1)$
$x^8 - 4x^7 - 4x^6 + 14x^5 + 23x^4$ $- 13x^3 - 32x^2 - 6x + 4$	81051965432	636704	1	v3109$(-2, 3)$

Table 9: Nonadic fields

field	$-D$	a	b	manifold
$x^9 - 3x^8 - 2x^7 + 11x^6 - 5x^5$ $- 10x^4 + 11x^3 + x^2 - 4x + 1$	8843652791	571	1	m115$(-5, 2)$
$x^9 - 3x^8 - 4x^7 + 16x^6 + x^5$ $- 22x^4 + 6x^3 + 4x^2 - 4x + 4$	48502810352	5230	1	v3157$(+5, 1)$
$x^9 - 3x^8 - 3x^7 + 13x^6$ $- 13x^4 + 2x^3 - 2x^2 + 3x + 1$	99961920379	15436	1	s649$(-5, 3)$

Table 10: Decadic fields

field	$-D$	a	b	manifold
$x^{10} - 4x^8 - 5x^7 + 5x^6 + 19x^5$ $- 2x^4 - 21x^3 + x^2 + 6x - 1$	271488204251	3669	1	m006$(-5, 2)$
$x^{10} - 4x^9 - x^8 + 20x^7 - 15x^6 - 23x^5$ $+ 29x^4 - 4x^3 - 7x^2 + 6x - 1$	7748687650003	232080	1	s900$(+2, 3)$

Table 11: Endecadic field

field	$-D$	a	b	manifold
$x^{11} - 3x^{10} - 5x^9 + 20x^8 + 3x^7 - 42x^6$ $+ 14x^5 + 28x^4 - 17x^3 - x^2 + 4x - 1$	21990497831723	68838	1	m007$(-5, 2)$

Table 12: Duodecadic field

field	$-D$	a	b	manifold
$x^{12} - 3x^{11} - 8x^{10} + 17x^9$ $+ 27x^8 - 19x^7 - 50x^6 - 24x^5$ $+ 44x^4 + 37x^3 - 5x^2 - 8x - 1$	12476239474594496	9408656	1	v2824$(+4, 1)$

35

Table 13a: Rational relations of Dedekind zeta values to volumes

$-D$	n	a	b	$\mathcal{M}$	vol($\mathcal{M}$)
23	3	1	1	m003$(-3,1)$	0.9427073627769277209213299603
283	4	1	1	m003$(-2,3)$	0.9813688288922320880914521899
3	2	2	1	m007$(+3,1)$	1.0149416064096536250211202554
331	4	1	1	m003$(-4,3)$	1.2637092386580436558847163346
59	3	4	1	m004$(+6,1)$	1.2844853004683544424603370884
7215127	7	46	1	m004$(+1,2)$	1.3985088841508066405096432426
23	3	2	3	m009$(+4,1)$	1.4140610441653915813819494040
365263	6	26	1	m004$(+3,2)$	1.4406990067273648752823700223
3998639	7	17	1	m004$(+5,2)$	1.5294773294300262628249286294
4511	5	1	1	m003$(-5,3)$	1.5435689114718550743284729436
31	3	1	1	m007$(+4,1)$	1.5831666660624812836166028851
44	3	2	1	m006$(+3,1)$	1.5886466393001629881769138120
3685907	7	14	1	m006$(-3,2)$	1.6496097158086641207983958810
4903	5	1	1	m015$(+5,1)$	1.7571260291884513628747465936
9759	5	3	1	m007$(-3,2)$	1.8243443222029119612749572176
4	2	2	1	m009$(+5,1)$	1.8319311883544380301092070296
29963	5	16	1	m007$(-5,1)$	1.8435859723266779387204547540
23	3	1	2	m016$(-3,2)$	1.8854147255538554418425992064
17348	5	8	1	m006$(-5,1)$	1.9415030840274677937303201270
283	4	1	2	m006$(+2,3)$	1.9627376577844641761829043794
10407	5	3	1	m023$(-4,1)$	2.0143365837768425042788264770
271488204251	10	3669	1	m006$(-5,2)$	2.0288530914749228457970677560
3	2	1	1	m036$(-3,2)$	2.0298832128193072500424051080
448	4	1	1	m010$(+3,2)$	2.0584843681930333624560507390
21990497831723	11	68838	1	m007$(-5,2)$	2.0656708348838074157630793200
5519	5	1	1	m016$(+3,2)$	2.1145676931102222380902130310
8647	5	2	1	m016$(+4,1)$	2.1340163368014215078604548000
238507	6	7	1	m034$(+4,1)$	2.1847555750625883970263246000
83	3	4	1	m034$(-3,2)$	2.2076662387269329124749198170
215811	6	6	1	m015$(-3,2)$	2.2267179039193896836178405510
7729991	7	32	1	m038$(+1,2)$	2.2597671325959755720567283600
5783	5	1	1	m016$(+2,3)$	2.2726318635865581745541504210
1588	4	8	1	m038$(+4,1)$	2.2779594449369265522793290570
275	4	2	5	m016$(-4,3)$	2.3430171369013062653562453240
23	3	2	5	m019$(+1,4)$	2.3567684069423193023032490070
2151	4	12	1	m015$(+8,1)$	2.3627007925545004764965958230
31	3	2	3	m149$(+1,2)$	2.3747499909372192542490432770
688	4	2	1	m019$(+3,4)$	2.4255853786663687835291635260
491	4	1	1	m029$(-3,2)$	2.4682321966809086789285230050
202734487	8	100	1	m038$(+3,2)$	2.5026593053728211155963957080

Table 13b: Rational relations of Dedekind zeta values to volumes

$-D$	n	a	b	$\mathcal{M}$	vol($\mathcal{M}$)
331	4	1	2	m070($-3, 1$)	2.5274184773160873117769432693
59	3	2	1	m039($+6, 1$)	2.5689706009367088849206741169
507	4	1	1	m160($-3, 2$)	2.5953875936867421383011993834
32775179	7	316	1	m026($-5, 2$)	2.6091812395130333623901936011
4795631	7	13	1	m032($+5, 2$)	2.6294053952883987222788830854
4903	5	2	3	m034($-5, 2$)	2.6356890437826770443121198971
7	2	4	1	m036($-4, 3$)	2.6667447834490579790796712462
58360112	7	788	1	m034($+5, 2$)	2.6794758057553125977970425681
751	4	2	1	m081($-4, 1$)	2.7818339123960797918753378021
1156	4	4	1	m082($+1, 3$)	2.7868045564155685218555094291
12558899	7	68	1	m070($-3, 2$)	2.8125164965432103731756174621
23	3	1	3	m221($+3, 1$)	2.8281220883307831627638988091
4297259	7	10	1	m221($-1, 2$)	2.9133321143060669356871934841
1192	4	4	1	m148($-3, 2$)	2.9215114289293830820040601131
283	4	1	3	m130($-2, 3$)	2.9441064866766962642743565691
848	4	2	1	m207($-1, 3$)	2.9583728675913943476361300751
60803	5	28	1	m148($+5, 1$)	2.9703211101889364287253537621
3	2	2	3	m149($-4, 1$)	3.0448248192289608750636076621
3998639	7	17	2	m286($-4, 1$)	3.0589546588600525254985725911
563	4	1	1	m130($-4, 1$)	3.0593380577789556733388096251
4511	5	1	2	m119($+3, 2$)	3.0871378229437101486569458861
7031	5	1	1	m160($-4, 1$)	3.1048085226800100910514729451
8843652791	9	571	1	m115($-5, 2$)	3.1232738281393185651851179041
58064	5	40	1	m141($+2, 3$)	3.1333496486608963513717969121
331	4	2	5	m146($+5, 1$)	3.1592730966451091397117908671
31	3	1	2	s119($+4, 1$)	3.1663333212496256723320577031
44	3	1	1	m141($+4, 1$)	3.1772932786003259763538276241
11243	5	2	1	s090($+5, 1$)	3.2529080484716459238073550631
107	3	4	1	m168($-3, 2$)	3.2758716439439339423695603701
3685907	7	7	1	m222($+3, 2$)	3.2992194316173282415967917631
23	3	2	7	m178($-2, 3$)	3.2994757697192470232245486101
1290496	6	80	1	m285($-4, 1$)	3.3410022008795375912267676031
463471	6	16	1	m249($+4, 1$)	3.3620932044270480437075892781
899447	6	44	1	m189($+3, 2$)	3.3831978936505561203563353051
7463	5	1	1	m178($+4, 3$)	3.4029912511664557525748947191
5783	5	2	3	m175($-1, 3$)	3.4089477953798372618312256321
2068	4	8	1	m389($+3, 1$)	3.4101879365720923770012101251
283	4	2	7	m189($-5, 2$)	3.4347909011228123083200826641
976	4	2	1	m286($-5, 1$)	3.4543139174920319063744203741
753079	6	26	1	m337($-3, 1$)	3.4742477613127422960290085531

Table 13c: Rational relations of Dedekind zeta values to volumes

$-D$	n	a	b	$\mathcal{M}$	$\mathrm{vol}(\mathcal{M})$
23103	5	6	1	m223$(+5,1)$	3.4763756733918128785629823202
4903	5	1	2	m220$(+5,2)$	3.5142520583769027257494931878
11551	5	2	1	m223$(-1,3)$	3.5440817346445798688845054424
2803244	6	236	1	m192$(-5,2)$	3.5504301411816643756523397631
81589747	7	828	1	m213$(-5,2)$	3.5736001480514123848358509401
643	4	1	1	m247$(-1,4)$	3.5817073255683653051422721521
92779	6	1	1	m222$(-6,1)$	3.6086890617707849435224972911
4	2	1	1	s942$(-2,1)$	3.6638623767088760602184140591
1399	4	4	1	m293$(+2,3)$	3.6756456059498707311628187401
29963	5	8	1	m310$(+1,2)$	3.6871719446533558774409095091
94363	6	1	1	m345$(+1,2)$	3.7028973218569406126163934431
1014119	6	38	1	m286$(-6,1)$	3.7199776543425777110728233531
104	3	4	1	s297$(+1,3)$	3.7588449482372842714332581001
23	3	1	4	s645$(-2,1)$	3.7708294511077108836851984121
331	4	1	3	s254$(+5,1)$	3.7911277159741309676541490401
59	3	4	3	s296$(-5,1)$	3.8534559014050633273810112541
17348	5	4	1	s403$(-1,2)$	3.8830061680549355874606402551
283	4	1	4	m339$(-2,3)$	3.9254753155689283523658087591
112919	5	88	1	m304$(+1,3)$	3.9339506377840332494265502951
76	3	2	1	s784$(+1,2)$	3.9702896238906553940104695581
12447	5	2	1	s657$(-1,2)$	3.9781278523591315263678733611
38083	5	14	1	s437$(+1,3)$	4.0039791545288820881837828581
1099	4	2	1	s663$(+1,2)$	4.0188172383616703515025279381
10407	5	3	2	m322$(+3,2)$	4.0286731675536850085576529541
6724	4	64	1	s479$(-5,1)$	4.0439868943131865222805611661
271488204251	10	3669	2	s394$(+5,2)$	4.0577061829498456915941355131
3	2	1	2	s912$(+0,1)$	4.0597664256386145000848102171
629952	6	18	1	s386$(+5,2)$	4.0611018452427859443439387271
448	4	1	2	s566$(+2,3)$	4.1169687363860667249121014791
1107052	6	50	1	v1315$(-4,1)$	4.1566754268179428917307386891
13219	5	2	1	s645$(+1,3)$	4.1713204013225000744474028351
751	4	4	3	s850$(-3,1)$	4.1727508685941196878130066701
66467451	7	480	1	s523$(-6,1)$	4.2010304150317892073479234421
5519	5	1	2	s648$(+5,1)$	4.2291353862204444761804260621
161939	6	2	1	s682$(+3,1)$	4.2302168347838973002857467841
23	3	2	9	s702$(-3,1)$	4.2421831324961747441458482131
87	3	2	1	s784$(-1,2)$	4.2525829469543476127927248021
1825672	6	100	1	m358$(-5,3)$	4.2596291312482915800639335251
8647	5	1	1	v0940$(-5,2)$	4.2680326736028043015720909601
400	4	2	5	m400$(+4,1)$	4.3062076007308086529198371591

Table 13d: Rational relations of Dedekind zeta values to volumes

$-D$	n	a	b	$\mathcal{M}$	vol($\mathcal{M}$)
365263	6	26	3	s961(+1, 2)	4.3220970201820946258471106669
104483	6	1	1	s648(+1, 2)	4.3300995083775460932348514667
238507	6	7	2	s649(−4, 1)	4.3695111501251767940526492011
4297259	7	20	3	s730(−1, 2)	4.3699981714591004035307902206
29444	5	8	1	s478(−1, 3)	4.3749665119836051914461454441
1968	4	6	1	s594(+1, 3)	4.4031550166948581009984336421
83	3	2	1	s869(−1, 2)	4.4153324774538658249498396355
283	4	2	9	s650(−1, 3)	4.4161597300150443964115348544
331	4	2	7	m400(+4, 3)	4.4229823353031527955965072135
50052727	7	296	1	v2200(−3, 2)	4.4544530844859249954764466577
116	3	4	1	s881(−1, 3)	4.4646589115486807720539326925
7729991	7	16	1	s645(+4, 3)	4.5195342651919511441134567215
5783	5	1	2	v2203(+3, 1)	4.5452637271731163491083008435
1588	4	4	1	v2641(−4, 1)	4.5559188898738531045586581145
79952	5	36	1	s594(+3, 2)	4.6064691524449498897457520265
22331	5	4	1	s884(+2, 3)	4.6110242618956380507098085035
731	4	1	1	s649(−3, 4)	4.6265650912775396154664681285
4511	5	1	3	s646(+5, 2)	4.6307067344155652229854188295
75117248	7	616	1	v1788(+3, 2)	4.6463299511446898123977437855
1107	4	2	1	s928(+4, 1)	4.6622892909473710768257469095
99961920379	9	15436	1	s649(−5, 3)	4.6787430722151433220161714235
141791	5	104	1	s707(+5, 1)	4.6822186293861196919372456025
275	4	1	5	v1251(+4, 3)	4.6860342738026125307124906495
23	3	1	5	s944(−1, 2)	4.7135368138846386046064980155
2151	4	6	1	s882(+4, 1)	4.7254015851090009529931916475
31	3	1	3	s874(+4, 1)	4.7494999818744385084980865555
44	3	2	3	v1368(+2, 3)	4.7659399179004889645307414375
2095218667	8	2240	1	s901(−3, 2)	4.8093670336024696521099582015
14103	5	2	1	s784(+5, 2)	4.8147680238800289287262973115
688	4	1	1	s944(−3, 2)	4.8511707573327375670583270525
31684	5	8	1	v2381(+3, 1)	4.8688568510980632008269566635
1879	4	4	1	v2914(+2, 3)	4.8757581591061572393562959095
11243	5	4	3	v2447(+1, 3)	4.8793620727074688857110325955
9429911	7	20	1	s838(−2, 3)	4.8833869715394765505639873755
283	4	1	5	v3215(+3, 1)	4.9068441444611604404572609485
239639	5	184	1	s918(+3, 2)	4.9240747510998012773060014355
491	4	1	2	s900(−1, 3)	4.9364643933618173578570460105
3685907	7	14	3	v2335(+3, 2)	4.9488291474259923623951876455
6515927	7	11	1	s900(+3, 2)	4.9530103681366797424729185405
23339	5	4	1	v3199(+3, 1)	4.9672417782154423052003228175

Table 13e: Rational relations of Dedekind zeta values to volumes

$-D$	n	a	b	$\mathcal{M}$	vol($\mathcal{M}$)
5873596	6	688	1	v1858(+6, 1)	4.98880955174336554075832256
948381887	8	496	1	v2486(−3, 2)	4.98980490778588582667165309 2
7557047	7	14	1	v2221(−1, 3)	5.00205329278997118662220015 9
202734487	8	50	1	s900(+1, 3)	5.00531861074564223119279141 6
331	4	1	4	v2402(+3, 2)	5.05483695463217462353886538 7
2401259831	8	1978	1	v3184(+4, 1)	5.05671803914258347935993930 1
3	2	2	5	v2422(+1, 3)	5.07470803204826812510601277 1
7463	5	2	3	v2344(+5, 2)	5.10448687674968362886234207 9
7748687650003	10	232080	1	s900(+2, 3)	5.10922754154802285188446440 3
14631	5	2	1	s958(+3, 2)	5.11272455819980858171190472 1
59	3	1	1	v3066(+1, 2)	5.13794120187341776984134833 9
43210364	7	242	1	v3305(−1, 2)	5.17242876869790618683508152 0
709783	6	20	1	s952(−4, 1)	5.17523058259697761090684335 0
507	4	1	2	v3347(+3, 1)	5.19077518737348427660398766 8
12476239474594496	12	9408656	1	v2824(+4, 1)	5.19421457152011204451489554 9
139	3	4	1	v3106(+3, 1)	5.19843366044256112540341032 8
9439	5	1	1	v2759(−3, 1)	5.20072371364459390339831190 4
1732	4	4	1	v3187(−4, 1)	5.20249684248082331112902946 4
32775179	7	158	1	v2725(−4, 1)	5.21836247902606672478038720 2
46692071	7	250	1	v2825(−4, 1)	5.24017030245476390597900883 1
14911	5	2	1	v2704(−5, 1)	5.26243610131190829211220971 8
4903	5	1	3	s944(−5, 2)	5.27137808756535408862423978 0
13523	5	2	1	v2530(+1, 3)	5.28793627052612713561228536 7
70736	5	32	1	v2787(−1, 3)	5.28893750721863751404954225 7
7	2	2	1	v3390(+3, 1)	5.33348956689811958159342492 5
58360112	7	394	1	v3462(−1, 2)	5.35895161151062519559408513 6
1791	4	4	1	s961(+2, 3)	5.36369322179598174418577776 7
7792864	6	976	1	v2789(−2, 3)	5.38725376465689000625517336 7
34779	5	9	1	v3214(+3, 1)	5.42676422712309899153781717 7
9759	5	1	1	v3031(+3, 1)	5.47303296660873588382487165 3
4	2	2	3	v3412(+5, 1)	5.49579356506331409032762108 9
13883	5	2	1	v3310(+5, 1)	5.50474883781801349672573749 5
34436	5	8	1	v2794(−2, 3)	5.50967698925577537121576098
4241707	6	296	1	v3428(−4, 1)	5.51797852201250999335157095 4
31	3	2	7	v3091(−2, 3)	5.54108331218684492658110098 1
751	4	1	1	v3277(−2, 3)	5.56366782479215958375067560 4
1156	4	2	1	v3183(−3, 2)	5.57360911283113704371101885 8
688927	6	14	1	v3243(−3, 1)	5.57625962636003943109336082 7
12558899	7	34	1	v3520(+4, 1)	5.62503299308642074635123492 5
48502810352	9	5230	1	v3157(+5, 1)	5.64678958454479680102882510

Table 13f: Rational relations of Dedekind zeta values to volumes

$-D$	n	a	b	$\mathcal{M}$	$\mathrm{vol}(\mathcal{M})$
7729991	7	64	5	v3264(+4, 1)	5.6494178314899389301418209901
23	3	1	6	v3375(−3, 2)	5.6562441766615663255277797618
2319	4	6	1	v2944(−5, 2)	5.6718835435665641696084968093
81051965432	8	636704	1	v3107(+2, 3)	5.6838825561389871452896746573
331	4	2	9	v3438(−3, 1)	5.6866915739611964514812235603
1494223	6	56	1	v3036(+3, 2)	5.6872820546525962148907851493
3312	4	12	1	v3209(+2, 3)	5.7243880548200265946063053633
97569124	7	736	1	v3214(+2, 3)	5.7367950471426702777716270066
22424	5	4	1	v3246(−2, 3)	5.7450001044490366341659680027
365263	6	13	2	v3184(−3, 2)	5.7627960269094595011294808922
561863	6	10	1	v3239(+3, 2)	5.8041744000016770017465291143
1192	4	2	1	v3214(−4, 3)	5.8430228578587661640081202271
283	4	1	6	v3431(−2, 3)	5.8882129733533925285487131380
848	4	1	1	v3477(+4, 1)	5.9167457351827886952722601516
661831	6	16	1	v3361(+1, 3)	5.9201058986757829232005281477
1927	4	4	1	v3452(−5, 1)	5.9344638838994724974262252667
417467	6	13	2	v3375(−5, 2)	5.9998808413142562202283076517
10407	5	1	1	v3418(+6, 1)	6.0430097513305275128364794311
1371	4	2	1	v3489(+2, 3)	6.0874354579691043593533878391
3	2	1	3	v3492(−4, 1)	6.0896496384579217501272153258
107264	5	52	1	v3454(−5, 1)	6.1201785289873395744928920961
1255	4	2	1	v3492(+4, 3)	6.2234317195189076604235817306
13219	5	4	3	v3543(+1, 3)	6.2569806019837501116711042537
58064	5	20	1	v3526(+2, 3)	6.2666992973217927027435938258

Table 14: Further single-complex-place fields, from cusped manifolds

field	$-D$	a	b	manifold
$x^2 + 2$	8	2	1	v2787
$x^3 - x^2 - 2x - 2$	152	4	1	v3526
$x^4 - 3x^2 - 2x + 1$	1328	2	1	v2631
$x^4 - x^3 + x^2 - 6x - 4$	2375	4	1	v3545
$x^4 + 5x^2 - 3$	4107	15	1	v1143
$x^5 - 2x^4 + 3x^2 - 2x - 1$	7367	1	1	m052
$x^6 - x^5 - 2x^4 - x^3 + 3x^2 + 2x - 1$	303619	5	1	s281
$x^6 - x^5 - 2x^4 + 4x^3 - 10x^2 + 6x + 3$	13266363	1362	1	v1461
$x^7 - 2x^6 - 6x^5 + 9x^4 + 12x^3 - 9x^2 - 11x + 2$	161329612	1832	1	v3418
$x^8 - 4x^7 + 5x^6 - x^5 - 6x^4 + 9x^3 - 4x + 1$	74671875	12	1	m283
$x^8 - 3x^7 - x^6 + 4x^5 + 8x^4 - 4x^3 - 8x^2 + 1$	397538359	142	1	v2824
$x^8 - x^7 - 6x^6 + 8x^5 - 12x^3 + 23x^2 - 9x - 3$	2597840403	2853	1	s311

Table 15: Joins of quadratics

quartic join	n_1	$-D_1$	n_2	$-D_2$	a	b_1	b_2	manifolds
$x^4 - x^2 + 1$	2	3	2	4	2	2	1	m350$(-1,3)$
								m360$(-2,3)$
					1	1	1	s913, v2274
$x^4 - x^3 - x^2 - 2x + 4$	2	3	2	7	4	4	1	v2274$(\pm 4,1)$
$x^4 - 3x^2 + 4$	2	4	2	7	4	2	1	v1859$(\pm 3,1)$
								v1859$(\pm 1,3)$
								m314–5

Table 16: Joins of a quadratic and cubic

sextic join	n_1	$-D_1$	n_2	$-D_2$	a	b_1	b_2	manifolds
$x^6 - x^5 + x^4 - 2x^3 + x^2 + 1$	2	3	3	23	1	1	3	v2274$(\pm 3,2)$
$x^6 - x^5 - 3x^3 + 2x^2 + x + 1$	2	3	3	44	1	1	1	v2274$(\pm 6,1)$
								v2274$(\pm 2,3)$
$x^6 - 2x^4 - 2x^3 + 4x^2 + 2x + 1$	2	3	3	59	2	2	1	v2274$(\pm 1,2)$
								s636$(-1,4)$
								s618$(+1,4)$
$x^6 - 4x^4 + 4x^2 + 1$	2	4	3	59	2	1	1	s518$(-1,4)$
								s530$(-1,4)$
					2	2	1	v3066
$x^6 - 6x^4 - 5x^3 + 16x^2 + 8x + 8$	2	7	3	59	4	1	2	v3066$(\pm 4,1)$

Table 17: Joins of cubics

nonadic join	n_1	$-D_1$	n_2	$-D_2$	a	b_1	b_2	manifolds
$x^9 + 2x^7 - 2x^6 + 8x^5 + 4x^4$ $+ 11x^3 + 4x^2 - 1$	3	23	3	59	2	6	1	v3066$(\pm 3,2)$
$x^9 - 2x^7 - 5x^6 + 12x^5 + 8x^4$ $+ 15x^3 + 4x^2 + 2x - 1$	3	44	3	59	2	2	1	v3066$(\pm 2,3)$
								v3066$(\pm 6,1)$

Table 18: Joins of a quadratic and quartic

quartic $\subset$ octadic join	n_1	$-D_1$	n_2	$-D_2$	a	b_1	b_2	manifolds
$x^4 - 2x^3 + 2$	2	4	4	400	4	1	5	m135$(\pm 1, 4)$
$\subset x^8 - 2x^7 + 2x^6 + 2x^5 - 2x^4$					4	3	5	v1859$(\pm 4, 1)$
$\quad + 2x^3 + 2x^2 - 2x + 1$								v1859$(\pm 1, 4)$
					2	1	5	v2942–7
$x^4 - x^3 + x + 1$	2	7	4	448	8	1	8	m235$(-4, 1)$
$\subset x^8 + 4x^6 + x^4 - 6x^2 + 4$								m234$(-1, 3)$
								m305$(-4, 1)$
					4	1	4	s719$(+7, 1)$
								v1373$(-2, 3)$
					4	1	8	v3505–7
$x^4 - x^3 - x^2 + x + 1$	2	3	4	507	2	1	1	m023$(-5, 1)$
$\subset x^8 - x^7 + 2x^6 + 3x^5 - x^4$								m022$(+2, 3)$
$\quad + 3x^3 + 2x^2 - x + 1$								m038$(-5, 1)$
					1	1	1	s645$(-2, 3)$
								s646$(-2, 3)$
								s648$(-7, 1)$
								s649$(+2, 3)$
								v1809$(-4, 1)$
								m345
					1	2	1	v3461–2
$x^4 + x^2 - 2x + 1$	2	4	4	1156	4	4	1	v3318–9
$\subset x^8 + 5x^6 + 4x^4 + 5x^2 + 1$								
$x^4 - x^3 - 2x^2 + 3$	2	3	4	4107	30	45	1	s869
$\subset x^8 - 5x^6 + 28x^4 + 15x^2 + 9$								
$x^4 - 2x^3 - x^2 + 2x + 2$	2	4	4	6724	128	32	1	m135$(\pm 2, 3)$
$\subset x^8 + 13x^6 + 40x^4 + 52x^2 + 16$					128	96	1	v1859$(\pm 2, 3)$
								v1859$(\pm 3, 2)$
					64	32	1	v3431$(+3, 2)$
								v3217$(-5, 1)$
								v3213$(-5, 1)$
								v3212$(+4, 3)$
								v3209$(+4, 3)$
								v3210$(+5, 1)$
								v3387$(-2, 3)$
								v3207$(+5, 1)$
								v3208$(+4, 3)$
								s937–41
								v2573–6

Table 19: Numerical values of $Z_{|D|} := Z_K$ for imaginary-quadratic fields

$-D$	$Z_{|D|}$
3	2.0298832128193072500424051085490405718833786150 6059
4	3.6638623767088760602184140597295364430965974971 2668
7	10.666979133796239163186849850442600176393535554 21055
8	12.046092040094377647268378629233594230996058049 44499
11	16.591299694831750484059840133967801881633675040 42159
15	37.663366733575215011080525922337902315111626802 52581
20	50.447631113712560021134271036085565405146805668 30894
24	62.186074773835025951066627260582431129650637182 33095
39	165.57570369926833581678917631121833077904271386 139253
84	404.73628202464445448608555478460494570288401081 12927

Table 20: Volume of the cubical and octahedral links

114.53761145123629432244247247899362494357488082420429231250851942121127501027441161281234687892520994210465731806315800802898317703007023740929928250084586460283983651330082726940759968759702920660531531580759324150754143878837313712948751658431691717430937727841133186281238554163446935932192296526607326107112771661119421686609275663701557572434730495583461169092818889421389435922005281897761327874817807227028106979273268111131932115068656188198395150052388050376562205880510599247458256799584524852839534204871794340415879015640464651359451611963572469692860082732987481808679811121461979920456281889724342334221434128669470931589996733606682840288093494107303594494398978521250331659884338246445176418045818749671259042778815966192535387078065534456559325249699463539195471108141659664645617899682627682970247100159721685353632474114663301702672270100187695488026006616569740599305776784442031978242453545449110127124720872091116784894114077580409525758170311502822254452974913073005473499436496449238935962195345038925840994685392028824455606704321440339408645356126352871216806577797486353620425213800992134976726381671853648499562580833637684771634300374412233657977320603017962160600891712728475261553785251066094558318038414643901857672691389752575734455792451007575910156390208650947188833967267657781465159708870679410250100730596375308142295927032872882984281618897314660744965215852278007793547439090335284739905795279447511546662295828302397553270669345151953323312678338628375580543191357119567032974463991717386810594008970591015124896982801226879473447589093589206619826480243308268769061440129087213425401259432152762517028190291894688438422778108128374452570774106841177990575035583054992839794034527044721173256021542771843790614964484378350457573395586234797502023753051754562990

Table 21: Volume of the dodecahedral and icosahedral links

310.9131454258982418156066571340803789107179627546
953866539274933469897444244121311099739939975971507
986432697092658238329149784692497393510959482161155
113550280240757024151460361498765323894883929966945
789956365988157798923976701962012526567526838465485
488002717713034428389238045657725918365258697285408
432490136774475650635259481305444958716428597071563
611411064456886341052373960417941929693593205047721
241883423696109219688922860638080690138258781523046
741686874993431587456559598847908069771332650858675
650630654788112165890478712971506603197258231133476
635406600631855051223906905320944272074684653584725
667817894996050270455301963078167128747884976936056
715275992273025680729781457953624667345120482003278
540179777583942295500075515836342826234566607211990
453989775867832671557955314292042596402107654942833
400933783738914027487226496284336189977658205024561
995144895131108872052678900538182256286704026182535
081549522339738817785994375329737225307361207888119
695103987475584594170061905352501618742058331415740
167087505655268271543088098482928187061043663478707
803859734833469938155027249782592798258476150133197
683816714709105042553956102458379417142495796685978
885556943637012844570671457052123486586594246666829
685917274002954751171405818823103567284268799018922
126485963876821972831339401215816266262935688361101
821397595969743744268728618974261107237652543059816
554792820367995001108285779255452283544860924831805
226023355633588361784074552968702184547644390948427
990048684246905487343294129765769179994381163373346
810874896700915514580688308119967508389482981267982
511015711538776266890885010769054671647412218515570
351084450669269648832817408688375570237213868883258
453864263914425147198193809500775033230947560721000
905153519571355423

Table 22: Empirical reductions of Feynman orthoschemes to the values of Table 19

ψ_1	ψ_2	ψ_3	$S(\psi_1,\psi_2,\psi_3)$	ψ_1	ψ_2	ψ_3	$S(\psi_1,\psi_2,\psi_3)$	ψ_1	ψ_2	ψ_3	$S(\psi_1,\psi_2,\psi_3)$
0	0	0	Z_4	0	0	$\frac{\pi}{6}$	$\frac{5}{3}Z_3$	0	0	$\frac{\pi}{4}$	$\frac{1}{4}Z_8$
0	0	$\frac{\pi}{3}$	$\frac{2}{3}Z_4$	0	$\frac{\pi}{6}$	0	$\frac{5}{3}Z_3$	0	$\frac{\pi}{6}$	$\frac{\pi}{6}$	$\frac{5}{6}Z_4$
0	$\frac{\pi}{6}$	$\frac{\pi}{4}$	$\frac{1}{24}Z_{24}$	0	$\frac{\pi}{6}$	$\frac{\pi}{3}$	$\frac{5}{6}Z_3$	0	$\frac{\pi}{4}$	0	$\frac{1}{4}Z_8$
0	$\frac{\pi}{4}$	$\frac{\pi}{6}$	$\frac{1}{24}Z_{24}$	0	$\frac{\pi}{4}$	$\frac{\pi}{4}$	$\frac{1}{2}Z_4$	0	$\frac{\pi}{4}$	$\frac{\pi}{3}$	$\frac{1}{12}Z_8$
0	$\frac{\pi}{3}$	0	$\frac{2}{3}Z_4$	0	$\frac{\pi}{3}$	$\frac{\pi}{6}$	$\frac{5}{6}Z_3$	0	$\frac{\pi}{3}$	$\frac{\pi}{4}$	$\frac{1}{12}Z_8$
0	$\frac{\pi}{3}$	$\frac{\pi}{3}$	$\frac{1}{6}Z_4$	$\frac{\pi}{6}$	0	$\frac{\pi}{6}$	$\frac{1}{12}Z_{15}$	$\frac{\pi}{6}$	0	$\frac{\pi}{4}$	$\frac{1}{144}Z_{84}$
$\frac{\pi}{6}$	0	$\frac{\pi}{3}$	$\frac{1}{72}Z_{39}$	$\frac{\pi}{6}$	$\frac{\pi}{6}$	$\frac{\pi}{6}$	$\frac{1}{6}Z_{11}$	$\frac{\pi}{6}$	$\frac{\pi}{6}$	$\frac{\pi}{4}$	$\frac{1}{16}Z_{15}$
$\frac{\pi}{6}$	$\frac{\pi}{6}$	$\frac{\pi}{3}$	$\frac{3}{4}Z_3$	$\frac{\pi}{6}$	$\frac{\pi}{4}$	$\frac{\pi}{6}$	$\frac{5}{24}Z_7$	$\frac{\pi}{6}$	$\frac{\pi}{4}$	$\frac{\pi}{4}$	$\frac{5}{12}Z_4$
$\frac{\pi}{6}$	$\frac{\pi}{4}$	$\frac{\pi}{3}$	$\frac{1}{48}Z_{15}$	$\frac{\pi}{6}$	$\frac{\pi}{3}$	$\frac{\pi}{6}$	$\frac{1}{2}Z_3$	$\frac{\pi}{6}$	$\frac{\pi}{3}$	$\frac{\pi}{4}$	$\frac{5}{24}Z_3$
$\frac{\pi}{6}$	$\frac{\pi}{3}$	$\frac{\pi}{3}$	$\frac{1}{12}Z_3$	$\frac{\pi}{4}$	0	$\frac{\pi}{4}$	$\frac{5}{4}Z_3$	$\frac{\pi}{4}$	0	$\frac{\pi}{3}$	$\frac{1}{24}Z_{20}$
$\frac{\pi}{4}$	$\frac{\pi}{6}$	$\frac{\pi}{4}$	$\frac{1}{6}Z_8$	$\frac{\pi}{4}$	$\frac{\pi}{6}$	$\frac{\pi}{3}$	$\frac{5}{8}Z_3$	$\frac{\pi}{4}$	$\frac{\pi}{4}$	$\frac{\pi}{4}$	$\frac{1}{4}Z_4$
$\frac{\pi}{4}$	$\frac{\pi}{4}$	$\frac{\pi}{3}$	$\frac{1}{12}Z_4$	$\frac{\pi}{3}$	0	$\frac{\pi}{3}$	$\frac{1}{6}Z_7$	$\frac{\pi}{3}$	$\frac{\pi}{6}$	$\frac{\pi}{3}$	$\frac{1}{3}Z_3$

Table 23: Maximally symmetric knots to 10 crossings

Rolfsen	HTW	sym	invariant trace field	sig	D	a	b
4_1	a4.1	D_4	$x^2 - x + 1$	$[0,1]$	-3	1	1
5_2	a5.1	D_2	$x^3 - x^2 + 1$	$[1,1]$	-23	1	3
6_3	a6.1	D_4	$x^6 - x^5 - x^4 + 2x^3 - x + 1$	$[0,3]$	-10571	$\times$	$\times$
7_4	a7.6	D_4	$x^3 + 2x - 1$	$[1,1]$	-59	1	1
7_7	a7.1	D_4	$x^4 + x^2 - x + 1$	$[0,2]$	257	$\times$	$\times$
8_{18}	a8.12	D_8	$x^4 - 2x^3 + x^2 - 2x + 1$	$[2,1]$	-448	1	6
8_{21}	n8.2	D_2	$x^4 - x^3 + x + 1$	$[0,2]$	392	$\times$	$\times$
9_{35}	a9.40	D_6	$x^3 - 2x - 2$	$[1,1]$	-76	1	1
9_{40}	a9.37	D_6	$x^4 + 2x^2 - 2x + 1$	$[0,2]$	592	$\times$	$\times$
9_{48}	n9.6	D_6	$x^3 - x^2 + x + 1$	$[1,1]$	-44	1	3
10_{123}	a10.121	D_{10}	$x^4 - x^3 + x^2 - x + 1$	$[0,2]$	125	$\times$	$\times$
10_{157}	n10.42	D_4	$x^3 + x - 1$	$[1,1]$	-31	1	8

Table 24: Less symmetric non-alternating Dedekind-zeta knots

Rolfsen	HTW	sym	invariant trace field	sig	D	a	b
9_{49}	n9.8	D_3	$x^3 - x^2 + 1$	$[1,1]$	-23	1	10
10_{139}	n10.27	D_2	$x^4 - 2x - 1$	$[2,1]$	-688	1	1
10_{152}	n10.36	Z_2	$x^5 - 3x^3 - 2x^2 + 2x + 1$	$[3,1]$	-8647	1	2
10_{153}	n10.10	triv.	$x^5 - 2x^4 - 2x^3 + 4x^2 - x + 1$	$[3,1]$	-29963	4	1

Table 25: Maximally symmetric knots from 11 to 16 crossings

HTW knot	sym	invariant trace field	sig
a11.366	D_6	$x^6 - x^5 + 4x^4 - 3x^3 + 4x^2 - 2x - 1$	$[2,2]$
n11.126	D_3	$x^5 - x^4 + 3x^2 - 2x + 1$	$[1,2]$
n11.133	D_3	$x^5 - x^4 + x^2 - x + 1$	$[1,2]$
a12.503	D_6	$x^7 + 2x^5 + 2x^3 - x^2 - x - 1$	$[1,3]$
a12.561	D_6	$x^7 - 2x^5 - x^4 + 2x^3 + x^2 + x - 1$	$[1,3]$
a12.1019	D_6	$x^{10} - 2x^9 + 2x^8 - 2x^7 - 3x^6 + 7x^5$	
		$\qquad - 3x^4 - 2x^3 + 2x^2 - 2x + 1$	$[2,4]$
a12.1202	D_6	$x^8 - x^7 + x^6 + 3x^4 + x^2 - x + 1$	$[0,4]$
n12.555	D_8	$x^5 + x^3 - x^2 + 2x + 1$	$[1,2]$
n12.642	D_8	$x^3 - x^2 + x + 1$	$[1,1]$
a13.1786	D_8	$x^8 + 2x^6 - x^5 + 3x^4 - x^3 + x^2 - 2x + 1$	$[0,4]$
a13.4877	D_8	$x^6 + 4x^4 - x^3 + 4x^2 - 3x - 1$	$[2,2]$
n13.4051	D_6	$x^5 - x^4 - x^3 + x^2 + 3x + 1$	$[1,2]$
a14.19470	D_{14}	$x^6 - 2x^5 + 2x^4 - 3x^3 + 2x^2 - 2x + 1$	$[2,2]$
n14.13191	D_5	$x^4 - x^3 - 2x + 1$	$[2,1]$
n14.17159	D_5	$x^6 - 2x^5 + x^4 + x^3 + x^2 - 2x - 1$	$[2,2]$
a15.84903	D_{10}	$x^8 - 2x^7 + x^6 - 2x^5 + x^4 - 4x^3 + 6x^2 - 4x + 4$	$[2,3]$
a15.85262	D_{10}	$x^6 - 3x^4 - 4x^3 + x^2 + 6x + 4$	$[2,2]$
n15.99226	D_{10}	$x^7 - x^6 + 2x^5 - x^4 + 3x^3 - 3x^2 + 2x + 1$	$[1,3]$
n15.112310	D_{10}	$x^4 - 2x^3 + x^2 - 2x + 1$	$[2,1]$
a16.379778	D_{16}	$x^8 - 4x^7 + 6x^6 - 11x^4 + 16x^3 - 10x^2 + 4x - 1$	$[2,3]$
n16.1007813	D_9	$x^3 + x - 1$	$[1,1]$

Fig. 1: Alternating platonic link from light-by-light scattering
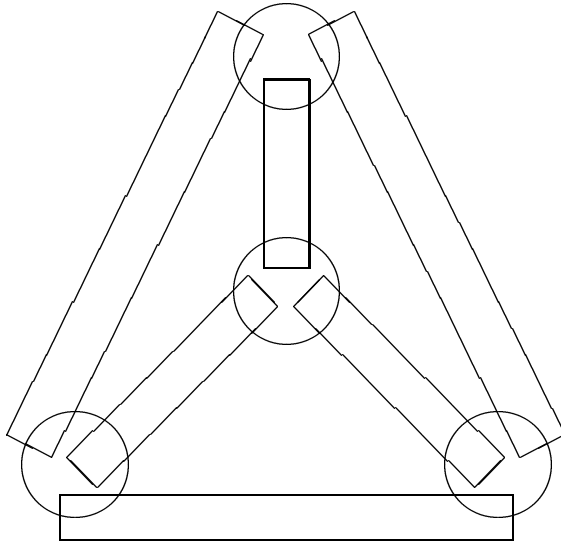

Fig. 2: Non-alternating daisy-chain link
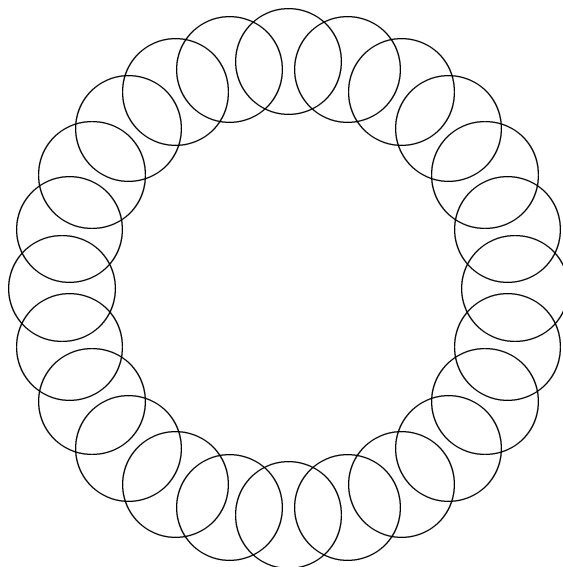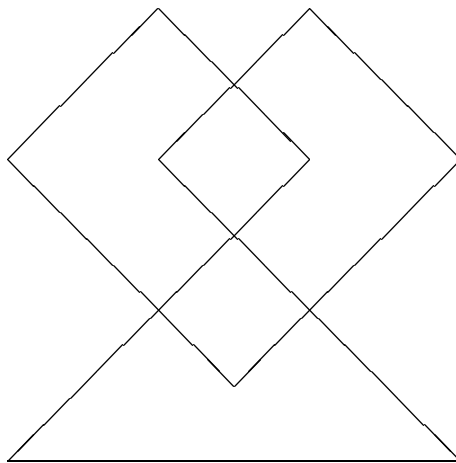

49

Fig. 3: Alternating figure-8 knot at $D = -3$
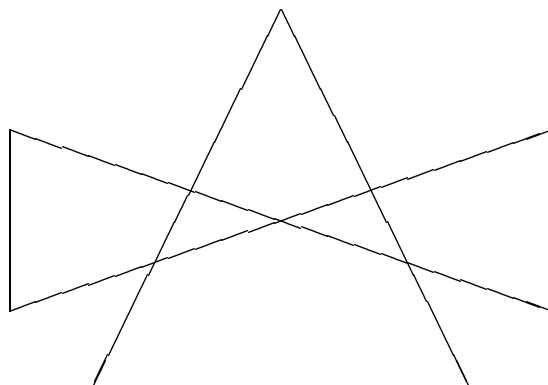

Fig. 4: Alternating Whitehead link at $D = -4$
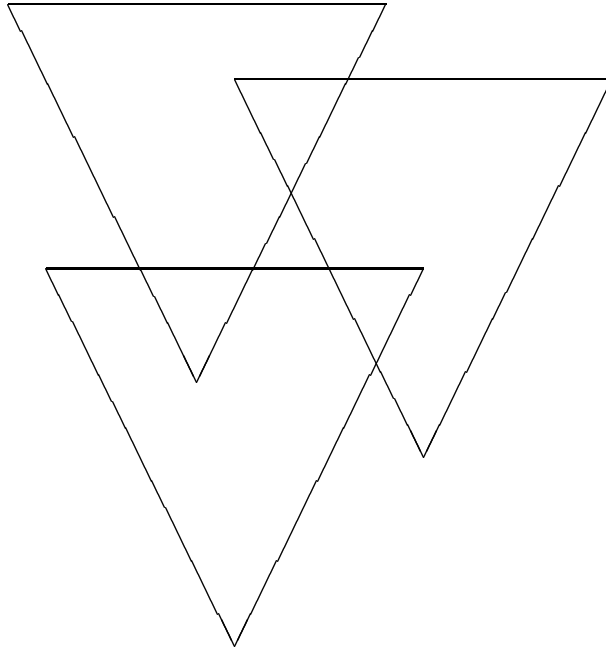
Fig. 5: Alternating link 6_1^3 at $D = -7$

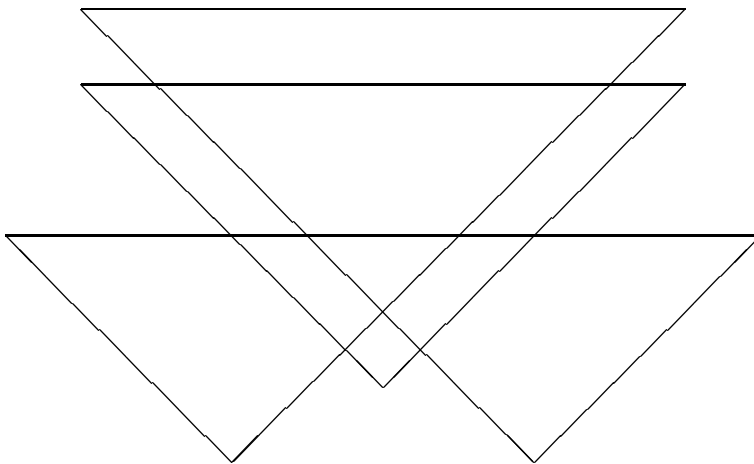**Fig. 6:** Alternating link 9_{40}^2 at $D = -8$